Report No. IDO-28552
AEC RESEARCH AND DEVELOPMENT REPORT
UC-81: Reactors Power
TID - 4500 (15th Edition)
Contract AT(10-1)-880

ARMY GAS-COOLED REACTOR SYSTEMS PROGRAM

INTERIM REPORT

IN-PILE TESTS OF GCRE-IB PROTOTYPE FUEL ELEMENTS

DECEMBER 1960

Aerojet-General NUCLEONICS
A SUBSIDIARY OF AEROJET-GENERAL CORPORATION
SAN RAMON, CALIFORNIA
THE GENERAL TIRE

LEGAL NOTICE

Report No. IDO-28552
AEC RESEARCH AND DEVELOPMENT REPORT
UC-81: Reactors Power
TID - 4500 (15th Edition)
Contract AT(10-1)-880

A R M Y G A S - C O O L E D R E A C T O R S Y S T E M S P R O G R A M

INTERIM REPORT
IN-PILE TESTS OF GCRE-IB PROTOTYPE FUEL ELEMENTS

H. T. Watanabe
J. E. Janne
W. D. Wilson

October 1960
(Report of work performed in 1958 - 1959)

Approved by:

G. A. Linenberger
Supervising Representative

Printed in USA. Price $2.00.
Available from the Office of
Technical Services, Department
of Commerce, Washington 25, D.C.

AEROJET-GENERAL NUCLEONICS
San Ramon, California
A Subsidiary of Aerojet-General Corporation

ACKNOWLEDGEMENT

Acknowledgement is made to Mr. G. W. Titus for his part as liaison engineer with Battelle Memorial Institute. The authors appreciate the contributions made by Mr. D. Keller of BMI and by his staff in the operation of the loop and post-irradiation hot cell evaluations.

DISTRIBUTION LIST

Category UC-81: Reactors - Power
TID 4500 (15th Edition)

Copies	
3	Aberdeen Proving Ground
1	Aerojet-General Corporation
35	Aerojet-General, San Ramon (IOO-800)
1	AFPR, Lockheed, Marietta
2	Air Force Special Weapons Center
2	ANP Project Office, Convair, Fort Worth
1	Alco Products, Inc.
1	Allis-Chalmers Manufacturing Company
10	Argonne National Laboratory
1	Army Ballistic Missile Agency
2	Army Chemical Center
1	Army Signal Research and Development Laboratory
1	AEC Scientific Representative , Argentina
1	AEC Scientific Representative, Belgium
1	AEC Scientific Representative, Japan
5	Atomic Energy Commission, Washington (Army Reactors Branch - 2 cys)
3	Atomics International
4	Babcock and Wilcox Company (NYOO - 1940)
3	Battelle Memorial Institute (D. Keller - 1 cy)
4	Bettis Plant
4	Brookhaven National Laboratory
1	Brush Beryllium Company
1	Bureau of Medicine and Surgery
1	Bureau of Ships (Code 1500)
1	Bureau of Yards and Docks
2	Chicago Operations Office
1	Chicago Patent Group
3	Combustion Engineering, Inc.
1	Convair-General Dynamics Corporation, San Diego
1	Defence Research Member
1	Denver Research Institute
2	Department of the Army, G-2
4	duPont Company, Aiken
1	duPont Company, Wilmington
1	Edgerton, Germeshausen and Grier, Inc., Las Vegas
1	Frankford Arsenal
1	General Atomic Division
2	General Electric Company (ANPD)
6	General Electric Company, Richland
1	General Nuclear Engineering Corporation
1	Gibbs and Cox, Inc.
1	Grand Junction Operations Office
2	Iowa State College
2	Jet Propulsion Laboratory
2	Knolls Atomic Power Laboratory
4	Los Alamos Scientific Laboratory
1	Mallinckrodt Chemical Works
1	Maritime Administration
1	Martin Company
1	Massachusetts Institute of Technology (Hardy)
1	Monsanto Chemical Company

DISTRIBUTION LIST (CONTINUED)

Copies

Copies	
1	Mound Laboratory
1	National Aeronautics and Space Administration, Cleveland
1	National Bureau of Standards
1	National Bureau of Standards (Library)
1	National Lead Company of Ohio
3	Naval Research Laboratory
1	New Brunswick Area Office
2	New York Operations Office
1	Nuclear Development Corporation of America
1	Nuclear Metals, Inc.
1	Oak Ridge Institute of Nuclear Studies
10	Office of Naval Research
2	Office of Naval Research (Code 422)
1	Office of Ordnance Research
1	Office of the Chief of Naval Operations
1	Office of the Surgeon General
1	Ordnance Tank-Automotive Command
1	Patent Branch, Washington
7	Phillips Petroleum Company (NRTS) (V. V. Hendrix - 1 cy)
1	Picatinny Arsenal
1	Power Reactor Development Company
3	Pratt and Whitney Aircraft Division
2	Public Health Service
1	Sandia Corporation, Albuquerque
1	Schenectady Naval Reactors Operations Office
1	Stevens Institute of Technology
1	Sylvania Electric Products, Inc.
1	Tennessee Valley Authority
1	Texas Nuclear Corporation
2	Union Carbide Nuclear Company (ORGDP)
7	Union Carbide Nuclear Company (ORNL) (A. L. Boch - 1 cy)
1	USAF Project RAND
1	U. S. Geological Survey, Albuquerque
1	U. S. Geological Survey, Denver
1	U. S. Geological Survey (Stringfield)
2	U. S. Naval Ordnance Laboratory
1	U. S. Naval Postgraduate School
1	U. S. Naval Radiological Defense Laboratory
1	U. S. Patent Office
2	University of California, Berkeley
2	University of California, Livermore
1	University of Puerto Rico
1	University of Rochester
2	University of Rochester (Marshak)
1	Walter Reed Army Medical Center
1	Watertown Arsenal
2	Westinghouse Electric Corporation (Schafer)
6	Wright Air Development Center
1	Yankee Atomic Electric Company
325	Technical Information Service Extension
75	Office of Technical Services, Washington
2	Engineer Research and Development Laboratories (J. A. Hughes - 1 cy)
1	Chief, California Patent Group

TABLE OF CONTENTS

TABLE OF CONTENTS (CONTINUED)

LIST OF TABLES

LIST OF FIGURES

(Continued)

LIST OF FIGURES (CONTINUED)

ARMY GAS-COOLED REACTOR SYSTEMS PROGRAM

INTERIM REPORT

IN-PILE TESTS OF GCRE-IB PROTOTYPE FUEL ELEMENTS

ABSTRACT

A program has been set up to develop and evaluate a ceramic-core, pin-type fuel element for the Army Gas-Cooled Reactor Systems Program. The method being used is to irradiate full-scale fuel elements in test loops (BRR-GCR, GETR, and ETR), under known reactor conditions. The experiment designated IB-IT, described in this report, was the first in a proposed series of tests. Two prototype elements were run in a gas-cooled loop in the Battelle Research Reactor. Average power generation of the elements was 30 kw. Irradiation times ranged from 35 to 165 hours. Results of the tests indicated that the enrichment of UO_2 in the outer circle of pins is close to the optimum value. The use of a finned surface on one of the test elements did not significantly increase the heat transfer properties. No significant distortions occurred in the elements as a result of thermal cycling.

I. INTRODUCTION

The objective of the experimental program discussed in this report was to obtain performance data on a ceramic-core, pin-type fuel element. Four specific areas were investigated: heat transfer, mechanical distortion, fluid flow, and fin effectiveness. To study this last property, two fuel elements, one with smooth pin surfaces and the other with finned pin surfaces, were irradiated to assess the effectiveness of an extended heat-transfer surface. A full-scale nuclear model was used to measure the flux distribution in the pin-type element.

The fuel element proposed for the ML-1 reactor* is the ceramic-core, pin-type. Because little is known about the high-temperature operation of such an element, a series of in-pile tests are being carried out under conditions simulating, as nearly as possible, those of the ML-1. The initial experiment is designated the IB-1T test series. This series evaluated two prototype fuel elements: IB-1αT and IB-1βT.

This experiment tested overall fuel element performance. Five factors were investigated: 1) fuel-pin surface temperature, 2) ceramic core temperature, 3) element power generation, 4) fluid-flow characteristics, and 5) the effects of thermal cycling.

To evaluate heat transfer rates, fluid flow characteristics, and temperature effects, two fuel elements were fabricated and instrumented with thermocouples. A full-scale nuclear mockup was instrumented with gold foils and flux wires to map the neutron flux distribution in the fuel element.

---

* Mobile, Low-Power Nuclear Reactor, being developed by Aerojet-General Nucleonics for the Army Gas-Cooled Reactor System Program.

Designation	Type	Purpose
IB-1αT	Smooth surface	Evaluate coolant flow, pressure drop in element, power produced by element
IB-1βT	Finned surface	Measure wall and liner temperatures, core temperature, and coolant gas temperature
IB-1ØT	Nuclear mockup	Determine flux distribution in the pin-type element.

II. EXPERIMENTAL APPARATUS

A. REACTOR LOOP

The tests were conducted in a gas-cooled loop designed and built by Battelle Memorial Institute. During operation the entire loop (a compact assembly consisting of a test section, preheater, heat exchanger, and blower) is immersed in the pool of the Battelle Research Reactor (BRR). This BRR-GCR loop was designed for the following conditions:

Coolant

Gas:	99.5% nitrogen + 0.5% oxygen
Pressure:	200 psia
Gas temperature:	
Inlet:	800°F
Outlet:	1400°F
Flow rate:	0.415 lb/sec max
Volume:	1.2 cu ft in loop
	1.0 cu ft static gas around blower
	6.0 cu ft in blower

Test Specimen

Power:	50 kw max
Pressure drop:	5 psi max
Thermal neutron flux:	5.4×10^{12} n/cm^2-sec
Gamma heating:	0.3 watts/gm

The loop can be controlled to vary the mass flow rate of the coolant, loop operating pressure, gas inlet temperature to the element, and the element power production.

Figure II-1 shows the longitudinal section of the loop assembly, and Figure II-2 shows the core and element arrangement. Complete descriptions of the loop have been reported by Battelle Memorial Institute.(1)

B. THE TEST FUEL ELEMENTS

1. IB-1αT Test Element

Figure II-3 shows assembly details of the IB-1α T fuel element. The element consisted of 19 fuel pins inside a 1.426-in.-dia zirconium inner liner. The inner liner was surrounded by rings of ceramic fiber insulating material (a combination of aluminum oxide and silicon oxide, marketed by Johns Mansville under the trade name Thermoflex). A 1.75-in. OD stainless steel outer liner was fitted over the insulated pin bundle. The outer liner was connected to a spacing sheet that supported and positioned the individual fuel pins. The 19 pins were arranged in the following configuration: an outer ring of 12 pins, each pin positioned on the corners of a dodecagon; a middle ring of 6 pins, each pin positioned on the corners of a hexagon; and a single pin in the center of the bundle.

Each fuel pin was fabricated of Inconel tubing, 0.225 in. OD by 0.163 in. ID. The total length of the pin was 32.78 in. The fueled length was 22.75 in. The fuel was in the form of compacted-and-sintered cylindrical pellets. The individual pellets were 0.1616 in. in diameter by 0.250 in. long. The 12 fuel pins in the outer ring of the element contained 25% enriched uranium; those in the intermediate ring and the center pin contained 50% enriched uranium. The ends of each pin were sealed by Heliarc welding, without the use of filler rods.

Fuel pins spacing was maintained by a network of spacers (bearings) with an airfoil-type cross-section. Forty spacers, located to provide maximum support to the pin bundle, were used in each fuel element. The spacers were attached to the outer walls of the pins by furnace-brazing. Nicrobraze-30 was used as the braze material.

2. IB-1βT Test Element

The general configuration of this element was similar to that of the IB-1αT element. Three modifications were made:

1. The heat-transfer (outer) surfaces of the pins were finned over a total length of 12 in., starting at a point 9.25 in. from the gas inlet end of the pin. The fin OD was 0.245 in.; the root diameter was 0.205 in.

(1) Numbers in parentheses refer to like-numbered items in the Bibliography at the end of this report.

2 The spacers were attached by spot welding instead of by brazing.

3 Each fuel pellet had a 0.048-in.-dia axial hole so that thermocouple wires could be inserted into the fueled regions of the element.

3. IB-1ØT Test Element

This element was a nuclear mockup of the foregoing two elements with identical pellets and tubing material, inasmuch as the element would operate at approximately room temperature (5 min at low power). The ends of the fuel pins were sealed with Epoxy resin, instead of by welding. Five of the fuel pins (Pins 1, 4, 7, 9 and 15, as shown in Figure II-4) contained a removable section (a ½-in.-long capsule) that could be withdrawn for counting fission product activity. These capsules were wrapped with a short piece of Mn-Cu wire to measure circumferential flux variations on a fuel pin. Nineteen Mn-Cu wires were inserted into axial holes drilled in the fuel pellets to measure axial flux distributions. In addition, flux monitor wires and gold foils were taped on the outside sleeve of the element for an absolute measure of neutron flux.

The fuel loading of each of the three elements is summarized below:

	Average U-235 Loading gm/in.		
Element	Outer 12 Pins	Inner 7 Pins	Total U-235 gm
IB-1αT	0.710	1.421	419
IB-1βT	0.653	1.275	380
IB-1 ØT	0.653	1.275	380

LONGITUDINAL SECTION OF BRR-GCR LOOP ASSEMBLY

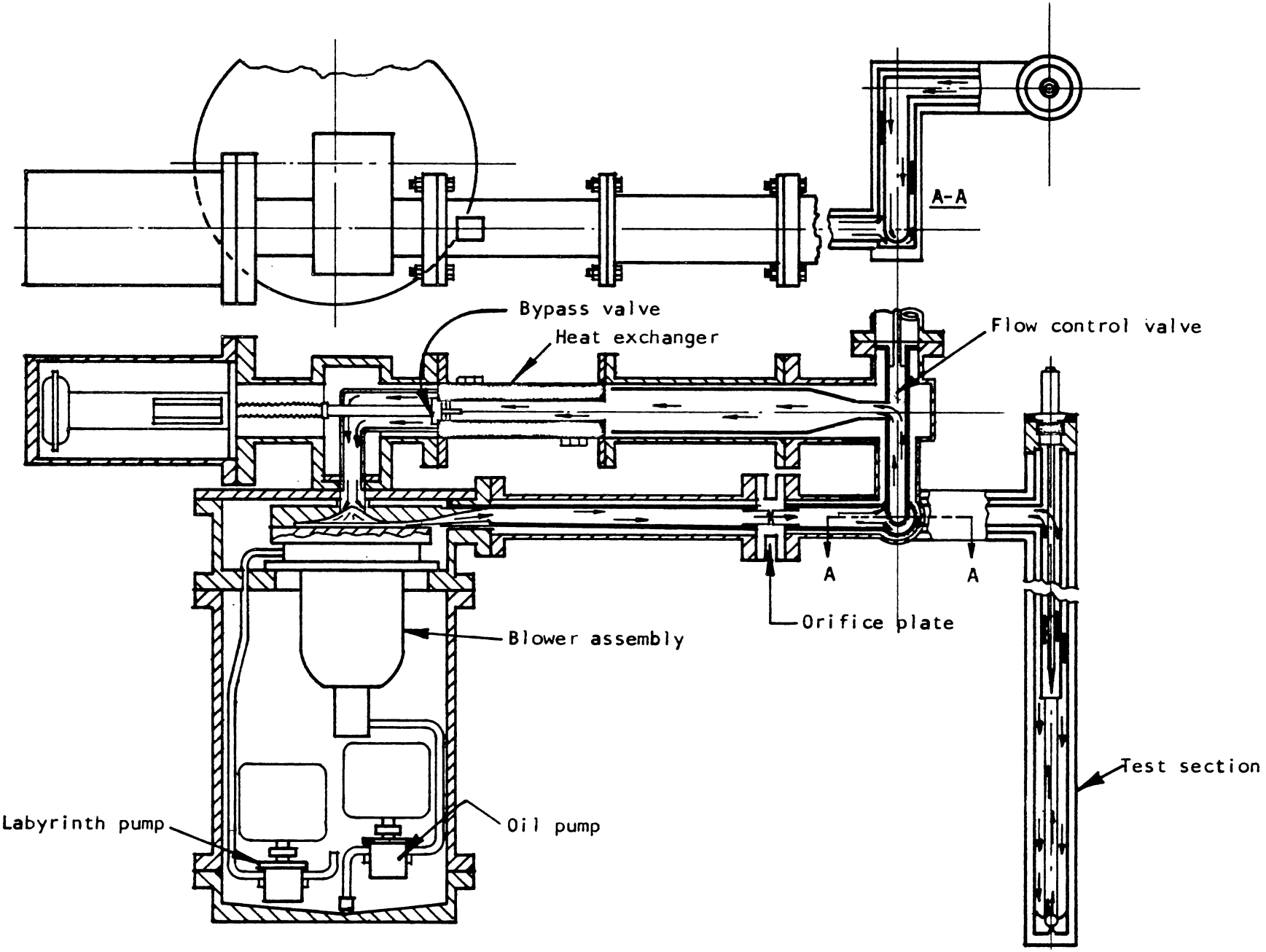

Figure II-1

CORE LOADING 10
GENERAL ARRANGEMENT

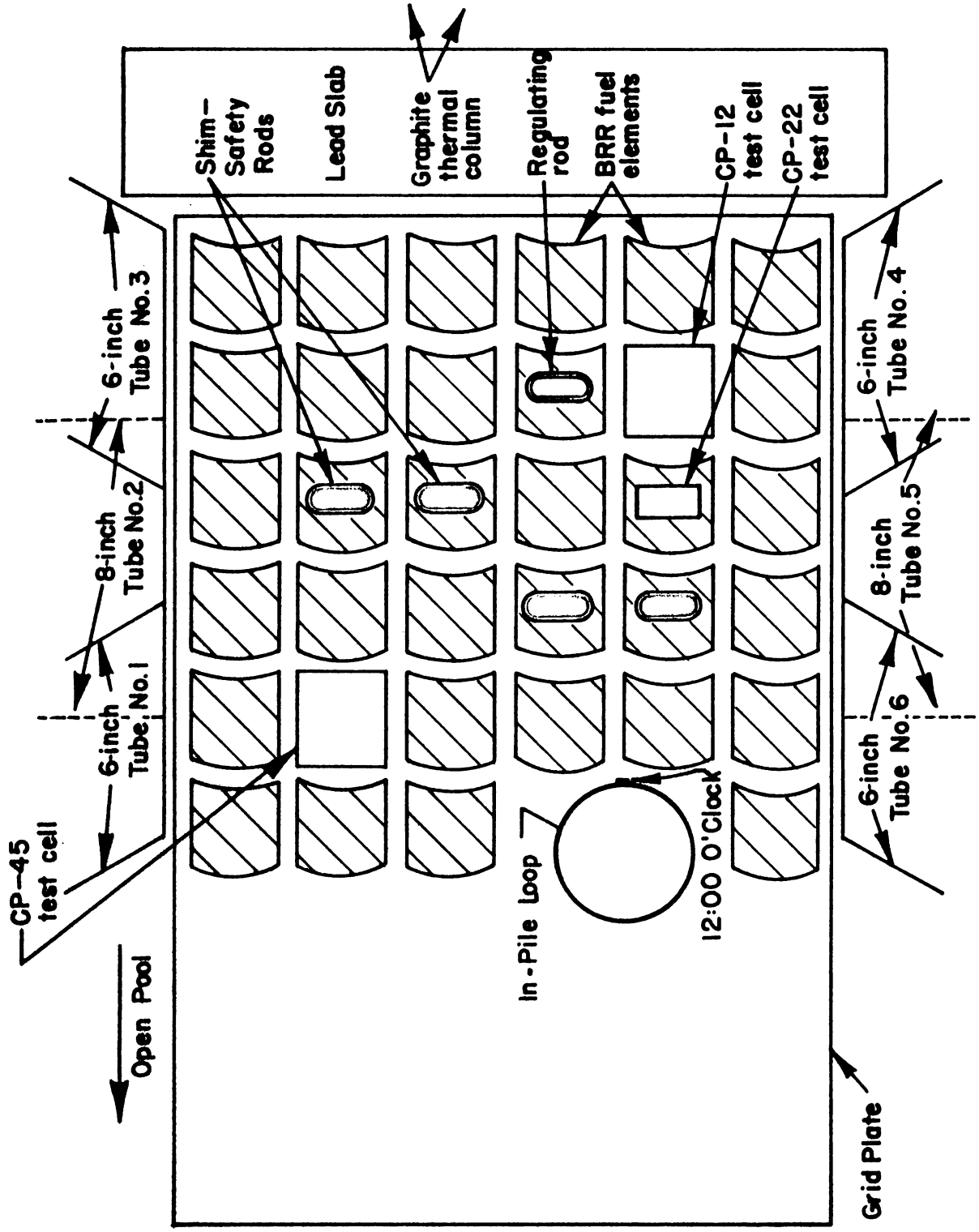

Figure 11-2

IB-IMT FUEL ELEMENT

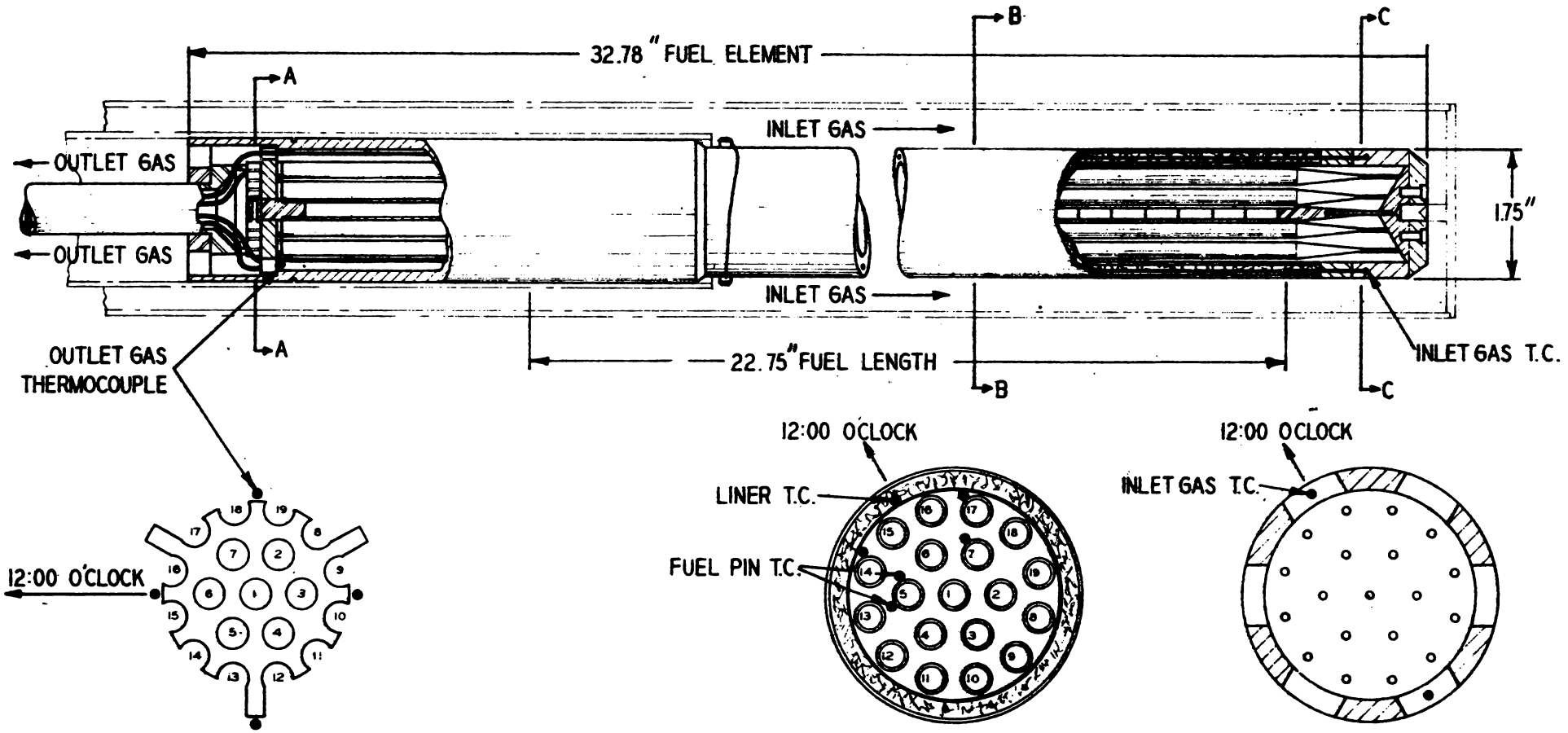

UPPER FUEL PIN HANGER
A-A

TYPICAL THERMOCOUPLE SECTION
B-B

LOWER FUEL PIN POSITIONER
C-C

Figure 11-3

CROSS SECTION
IB-IØT FUEL ELEMENT

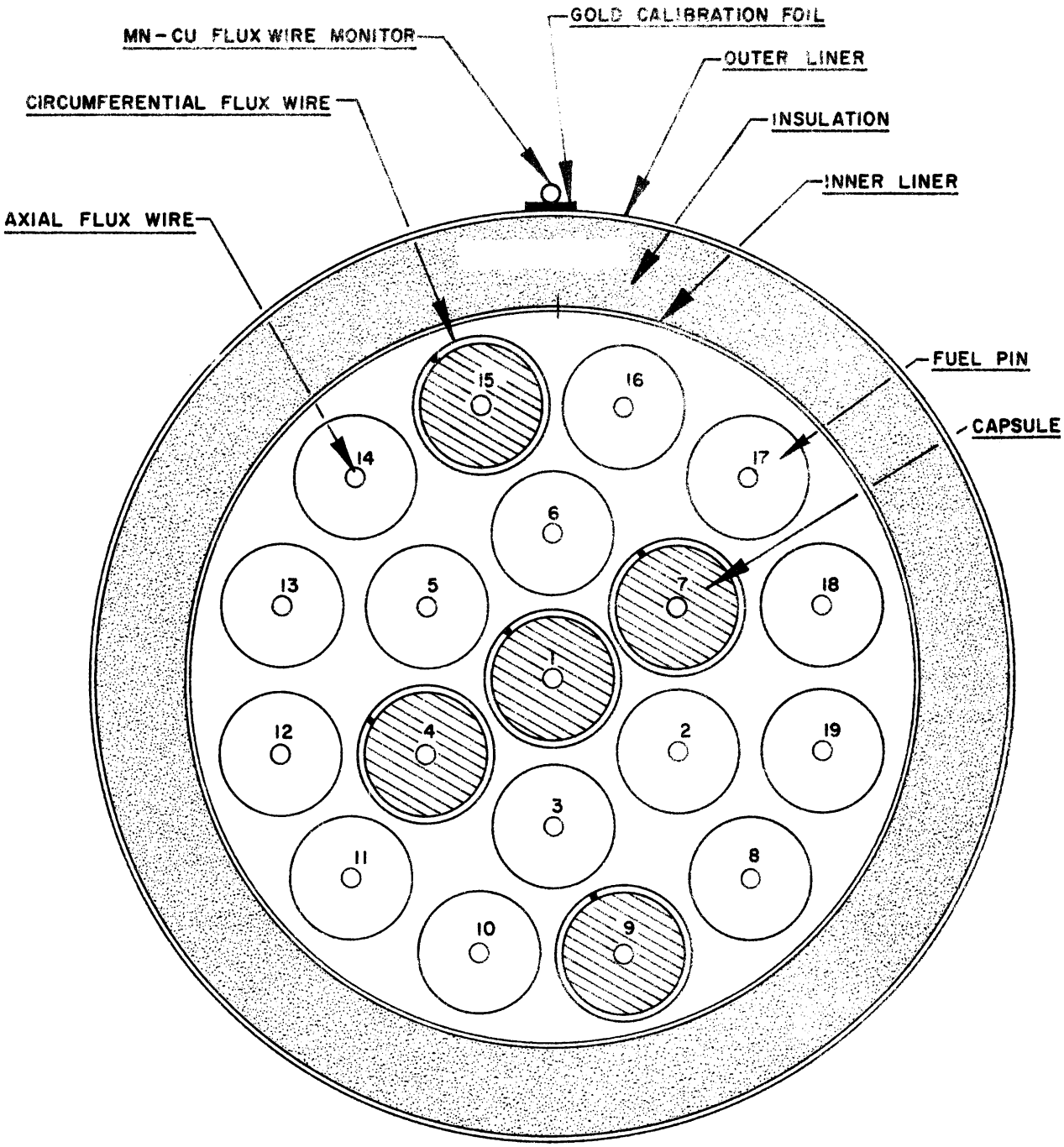

III. THE IB-1αT TEST ELEMENT

The IB-1αT element was tested for a total irradiation time of 165 hours between 23 June 1959 and 18 July 1959. Post-irradiation studies in the hot cell began on 19 August 1959.

There were no extended periods of steady-state operation at any one set of operating conditions. The principal cause of interruptions in the operation was the discovery of fission-product gases in the loop. When possible leaks were discovered in the fuel pins, operational procedures were instituted to permit a close check to be kept on the gas activity in the loop during subsequent operations.

The test was performed at nominal peak pin-surface temperatures of 1000°, 1100°, 1200°, 1350°, and 1500°F. Figure III-1 gives the operating history of the element. Shown are coolant gas temperatures, flow rate, pressure drop and element power as a function of time. The element was thermally cycled at a nominal rate of 10°F/sec for 252 cycles.

A. INSTRUMENTATION

1. Fuel Element

The IB-1αT element was instrumented to obtain temperature data on the coolant gas and fuel pin surfaces. The element was designed with 26 thermocouples, at locations tabulated in Table III-1 and shown in Figure III-2. The 12 o'clock position on the element points to the reactor face (see Figure II-2).

Sheathed, MgO-insulated thermocouples were used in the element. The sheathing material was Type-316 stainless steel, with a nominal wall thickness of 0.007 in. The chromel and alumel thermocouple wires were 0.005 in. in diameter.

Table III-1

POSITIONS OF IB-1αT THERMOCOUPLES

Thermocouple No.	Location on Pin No.	Temperature Measured	Axial Location on Element X/L	Junction Type
1	--	Inlet gas	Below 0	Closed-end
3	--	Outlet gas	Above 1.0	" "
4	--	" "	" "	" "
5	--	" "	" "	" "
6	--	" "	" "	" "
7	--	Inner liner	0.210	" "
8	--	" "	0.372	" "
9	--	" "	0.500	" "
10	--	" "	0.708	" "
11	--	" "	0.808	" "
12	--	" "	0.988	" "
13	1	Pin wall	0.850	Open-end
14	12	" "	0.203	" "
15	18	" "	0.542	" "
17	7	" "	0.850	" "
18	14	" "	0.850	" "
19	17	" "	0.878	" "
20	8	Periphery of pin	0.940	" "
21	8	" "	0.940	" "
22	8	" "	0.940	" "
23	--	Gas stream	0.952	Closed-end
24	--	" "	0.950	" "
25	--	" "	0.965	" "
26	5	Pin wall	0.850	Open-end

Table III-2, below, lists the thermocouples that failed during fabrication or irradiation. All of the thermocouples that failed during irradiation did so during, or shortly after, a thermal cycle.

Table III-2

INOPERATIVE IB-1 α T THERMOCOUPLES

Thermocouple No.	Location	Junction Type	Axial Location on Element X/L	Length of Operation Hours
1	Gas inlet	Closed-end	below 0.00	30
2	Gas inlet	Closed-end	0.00	Lost in fabrication
13	Pin No. 1	Open-end	0.80	116
14	" " 12	Open-end	0.20	27
15	" " 18	Open-end	0.50	116
16	" " 5	Open-end	0.85	Lost in fabrication
17	" " 7	Open-end	0.80	94
18	" " 14	Open-end	0.80	116
20	" " 8	Open-end	0.93	Damaged during element installation in loop
22	" " 8	Open-end	0.93	90
23	Gas stream, between Pins 1, 3, & 4	Closed-end	0.94	117
26	Pin No. 5	Open-end	0.80	117

2. Test Loop

The loop was instrumented to obtain information on: flow rate, loop pressure, element pressure drop, pool temperature, and reactor operating power. The coolant gas in the loop was continually monitored for radioactivity, and a sample was withdrawn periodically for analysis in a 100-channel gamma ray spectrometer. The loop instrumentation is shown in Figure III-3.

B. ELEMENT PERFORMANCE CHARACTERISTICS

1. Heat Transfer

Heat transfer information was obtained experimentally by measuring the surface temperature of the fuel pin and the inlet and outlet gas temperatures. The power generated by the fuel element was to be calculated from the flow rate, heat capacity, and increase in coolant temperature. However, after 30 hr of operation, the single operative inlet gas thermocouple of the fuel element failed. Thereafter, the power-generation calculation was based only upon the correlation between the fuel element gas inlet temperature, and the pre-heater outlet temperature. Thus, an uncertainty of $\pm$ 2 kw exists in this calculated value after 30 hours.

The operating temperature range of the IB-1αT test is shown in Figure III-4. This plot represents temperatures at the predicted hot spot (X/L = 0.88) on a pin in the outer ring.

The surface temperatures of five pins in the outer ring were measured at four different axial locations. The surface temperatures of the intermediate and center pins were determined from a measurement made at one axial position. Table III-3, on the following page, tabulates the measured and predicted temperatures for each thermocouple, at two typical operating conditions. The measured temperatures agree with the predicted temperatures within $\pm$ 65°F, less than a 6% deviation from the predicted values.

The predicted temperatures were calculated by using the IBM-704 code HECTIC.[2] This code is basically an energy balance between several coolant flow passages and several heated surfaces. For an arbitrary fraction of the total power generated in each surface, HECTIC calculates the coolant and surface temperatures as a function of the distance downstream from the inlet end of the fuel element, during steady-state operation. The unique feature of HECTIC is that turbulent exchange of fluid between several flow passages can be considered. In this case, each of the 19 pins was considered as a heated surface; the inner liner, as a non-heated surface. The element flow area was divided into 30 passages with 4 or 5 passages around each pin.

The calculated pin surface temperatures were based on experimental conditions of inlet gas temperature, element power generation, coolant flow rate and coolant pressure. The fractional power produced in each pin was also based on experimental data (see Section V, The IB-1ØT Test). The axial flux (and therefore axial power distribution) was modified somewhat from the experimental data to minimize the flux peak at the exit end of the element.

The measured temperature at X/L = 0.2 may be interpreted as indicating a low temperature, because a bearing spacer was located 0.4 in. upstream from the thermocouple. This bearing spacer caused turbulence immediately downstream and, therefore, induced greater heat transfer in the thermocouple region. When this turbulence is treated as

TABLE III-3

COMPARISON OF MEASURED AND PREDICTED TEMPERATURES

IB-1 T Element

70.1 Hours of Operation

Ring	Thermocouple Number	Axial Position (X/L)	Pin No.	Measured Temperature	Predicted Temperature	Difference (Meas. Less Pred.)	% Error (Difference / Predicted)
Outer	14	0.203	12	1040°F	1103°F	-63°F	5.71
Outer	15	0.543	18	1280	1262	+18	1.42
Outer	18	0.850	14	1340	1282	+58	4.52
Outer	19	0.878	17	1335	1270	+65	5.12
Outer	21	0.940	8	1203	1223	-20	1.64
Intermediate	26	0.850	5	1330	1312	+18	1.37
Intermediate		0.850	7	1287	1300	-13	1.00
Center	13	0.850	1	1310	1304	+6	0.46

40.5 Hours of Operation

Outer	14	0.203	12	740°F	790°F	-50°F	6.34
Outer	15	0.543	18	950	940	+10	1.07
Outer	18	0.850	14	995	953	+42	4.41
Outer	19	0.878	17	990	940	+50	5.32
Outer	21	0.940	8	850	892	-42	4.72
Intermediate	26	0.850	5	995	979	+16	1.64
Intermediate	17	0.850	7	960	966	-6	0.62
Center	13	0.850	1	955	970	-15	1.55

an entrance effect into a flow channel, the increase in heat transfer coefficient may vary between 20 and 60%.

Thermocouples attached to the outer surface of the inner liner measured bulk coolant temperatures. The temperatures followed the predicted axial temperature profile for the first 10 hr of operation, then drifted until all the thermocouples indicated a constant temperature. This leveling off was probably the result of the thermocouples short-circuiting near the top of the fuel region.

a. Circumferential Element Temperature

The radial temperature variation across the fuel element was measured in order to have a basis on which to establish the proper fuel loadings for later-model elements. Radial temperatures were measured at X/L = 0.85 on 4 pins (2 outer-ring pins, 1 intermediate-ring pin, and the central pin). There were wide fluctuations in the temperature of the rings, which made it difficult to determine the average temperature of the ring. Figure III-5 shows these temperature fluctuations during the longest period of steady-state operation (from the 65th to the 90th hour of irradiation). Nominally, the outer ring was operating approximately 15°F hotter than the intermediate ring, while the center pin was about 10°F cooler than the middle ring.

The temperature variation around the element at a position 6.5 in. above the fueled region was measured by the 4 outlet gas thermocouples. The thermocouple on the 12 o'clock side indicated a higher temperature than the 6 o'clock thermocouple; the temperature difference ranged between 30° and 95°F (see Figure III-6). Assuming a uniform inlet temperature, the bulk gas on the 12 o'clock side had a greater increase in temperature (by 11-23%) than did bulk gas on the 6 o'clock side.

HECTIC calculations predicted that the bulk gas temperature increase on the 12 o'clock side would be only 11 to 13% greater than that on the 6 o'clock side. The large variation that occurred in the experiment suggests that the amount of coolant mixing is less than that predicted by HECTIC, or that the thermocouples may not have been equally spaced in the gas stream.

b. Circumferential Pin Temperatures

The variation in temperature around an individual fuel pin was measured on a pin in the outer ring (Pin 8). This pin had two thermocouples attached at X/L = 0.94. One thermocouple was adjacent to the inner liner; the other was adjacent to the intermediate ring.

The side of the fuel pin nearer the liner operated 75° to 150°F cooler than the side nearer the intermediate ring. HECTIC predicted a maximum temperature difference of only 60° to 70°F around the pin. Figure III-7 shows much scatter in the measured temperature differences; this may have been caused by the bearing spacer on Pin 9 (adjacent to Pin 8) which was only 0.1 in. upstream from the thermocouple on Pin 8.

2. Fluid Flow

The predicted pressure drop across the IB-1αT test element was 20 to 35% greater than the measured pressure drop across the test section of the BRR loop. Figure III-8 shows the comparison between measured and predicted pressure drops, using friction factors derived from laboratory water flow tests.(3)

The predicted pressure drop used the following correlation:

$$\Delta P = \frac{f^* \; W^2 \; A}{\rho_m \; 2g_c \; A_c^3} + \frac{W^2}{A_c^2 \; g_c \alpha} \left(\frac{1}{\rho_o} - \frac{1}{\rho_i} \right)$$

Where:

P	=	pressure drop, lb/sq ft
W	=	coolant mass flow rate, lb/hr
A	=	surface area in contact with coolant, sq ft
A_c	=	cross sectional area for coolant flow, sq ft
ρ_m	=	average coolant density, lb/cu ft
ρ_i	=	entrant coolant density, lb/cu ft
ρ_o	=	exit coolant density, lb/cu ft
g_c	=	Newton's Law conversion factor, ft/hr^2
α	=	kinetic energy factor (varies between 0.90 and 0.94)
f^*	=	friction factor measured in water flow test, including the entrance and exit effects

Figure III-9 shows friction factors obtained from the water flow test and those derived from the experimentally measured pressure drop, using the above correlation.

C. COOLANT GAS ANALYSIS

Coolant gas samples were taken from the loop at intervals during the experiment and analyzed in a 100-channel gamma ray spectrometer. By comparing samples of known isotopes with the spectrometer gas sample, it was found that, after 50 hr of operation, the coolant gas contained some fission products. The major isotopes in the fission gas were Xe-133, Xe-135, and Kr-85m.

After 90 hr of operation the activity of the gas was checked at 2-hr intervals. Table III-4, below, lists loop gas activities and the associated loop operations.

Table III-4

LOOP GAS ACTIVITY DURING OPERATION OF THE IB-1∝T ELEMENT

Hours after Start of Operation	Loop Gas Activity (Millicuries)	Associated Loop Operation
94-108	Increased from 0 to 15	Held peak element temperature at 1200°F
108-115	Increased from 15 to 30	Held peak element temperature at 1200°F
115-123	Fluctuated between 20 and 30	Thermal cycling
123-143	Fluctuated between 12 and 25	Held peak element temperature at 1000°F
143-149	Increased from 25 to 52	Thermal cycling
149-152	Decreased from 52 to 40	Reduced peak element temperature from 1000°F to 750°F
152-162	Decreased from 40 to 18	Held peak element temperature at 750°F
162-164	Increased from 18 to 55	Performed 1 slow thermal cycle

The correlation between the pin surface temperature and the total activity in the loop during the slow thermal cycle is shown in Table III-5, below.

Table III-5

ACTIVITY AND TEMPERATURE OF IB-1α T ELEMENT

Time	Surface Temperature of Pin, °F	Total Activity in Loop, Millicuries
1110 hours	1000	33.0
1115 (start cycle)	1000	----
1125	1300	36.5
1133	1600	45.0
1139	1300	51.5
1145 (end cycle)	1000	----
1146	1000	54.5

Analysis of an exhaust gas sample taken at the end of this thermal cycle showed that the activity was above the maximum allowable limit at which the loop could be permitted to operate. The test was therefore terminated.

D. POST-IRRADIATION EVALUATION

The element was subjected to 272 thermal cycles during the irradiation period. Twenty of these cycles were caused by normal reactor operation; 252 were controlled thermal cycles. The nominal fuel pin surface temperature change during the thermal cycles was 10°F per second (see Figure III-10).

1. Mechanical Distortion

Distortion and mechanical displacement of the fuel pins were detected in several ways: 1) changes in gap spacing between individual pins and between rings of pins, as determined by differences in pre- and post-irradiation gap measurements; 2) bowing or twisting of pins, as determined by deviations from a flat surface; 3) "dimples" or bulges in the inner liner caused by spacers pressing into the liner, as detected by visual observation and photography; and 4) general visual observations.

Measurements were made on the completed IB-1α T fuel element just before final assembly. The amount of distortion was determined by comparing pre-irradiation data with those taken after irradiation. Figure III-11 shows the change in gap spacing at the two cross-sections where measurements were taken (X/L = 0.8 and 0.5). Three measurements were taken: 1) gap between the center pin and the line tangent to two adjacent outer ring pins, 2) gap between the intermediate ring pin and the line tangent to two adjacent outer ring pins, and 3) gap between adjacent outer ring pins.

The measurements were made with a special feeler gauge that indicated gap width on a plunger and dial arrangement. The gauge as it is being prepared for measurements is shown in Figure III-12.

A "flat surface" was placed next to the completed IB-1αT fuel element after irradiation to determine if there had been any bowing of the fuel element assembly. The surface of the outer liner was flush with the "flat surface" at any given angular position. After visual inspection and gap measurements, the pins were cut free from the upper support. The cutting was done with a hacksaw while the pin bundle was supported in a vise. Figure III-13 shows the IB-1αT pins after they had been separated from the upper support. The pins are arranged in sequence, with Pin 1 at the bottom and Pin 19 at the top.

Visual observations, gap measurements and bowing measurements all indicated that no significant amount of distortion had occurred in the element after 160 hr of operation at a nominal 30 kw.

Visual observation showed that the middle bearing spacer on Pin 16 was very badly corroded, and the corrosion had affected the three pins which were in contact with this spacer (Pins 15, 17, and 6). The pins were corroded on the surfaces facing the corroded bearing spacer, in a manner which suggested that a corrosive liquid may have boiled out of the spacer and splattered on the adjacent pins.

2. Fuel Pin Integrity

The element was leak-checked in the hot cell to determine the pin or pins that were releasing fission products (refer to Paragraph III, C, Coolant Gas Analysis). The leak-checking was performed by placing each fuel pin in a solution of dimethyl phthalate and drawing a vacuum over the liquid. Bubbles escaping from the fuel pin wall and rising through the liquid indicated the presence of leaks in Pins 16 and 15. Pin 16 leaked at the badly corroded bearing spacer which was attached to it, and Pin 15 leaked at the point where it contacted the corroded spacer.

3. Corrosion

Except for this one corroded spacer, the element did not appear to have been damaged by its in-pile exposure. Severe corrosion occurred only at this point, which was located at approximately the element hot spot (see Figures III-14, -15, and -16). During the hot cell examination, the spacer was sectioned. The section was made in such a way that only the leading surface of the spacer was removed. (This spacer was sectioned both longitudinally and transversely. All the photos were taken of the transverse section). Figures III-17, -18, and -19 illustrate the structures observed in this section.

Figures III-17 and -18 are photomicrographs of the Inconel spacer and underlying Inconel tubing. The spacer appears to have an as-cast structure, with pockets of braze material evident at the spacer-tubing interface. Voids at grain boundaries are evident in these photomicrographs, as is penetration of the grain boundaries by the braze

material. Figure III-19 illustrates heavy grain boundary precipitates found throughout this material. Figures III-17 and -18 also show transgranular cracking of the tubing material and a severely attacked spacer. The heavy precipitate evident in both the tubing and the spacer is not a characteristic of Inconel.

These peculiar occurrences indicated the possibility of mixed materials in the pin, in the spacer, or in both. Further investigations showed that some spacers have been severely attacked by the etchant used to clean the pins and spacers after brazing.

It was to determine whether mixed materials were present that the longitudinal section was made. In an effort to ascertain from what material the spacer had been fabricated, a spectrographic analysis was made. On the basis of this analysis, the spacer material was identified as Inconel. Its elemental constitution was within the limiting chemical compositions published by the supplier.

Figures III-20 and -21 illustrate typical structures in an uncorroded spacer. This spacer was on Pin 15. Figure III-20 shows the Inconel tubing and the spacer. Clearly evident is a precipitate, distributed through the entire structure and concentrated at grain boundaries. The white area is apparently a portion of the spacer that reacted sufficiently enough with the braze to remove all traces of grain boundaries in this zone. Both tubing and spacer are shown again in Figure III-21. An unbrazed point is obvious at the center of this view. Although there are voids in the spacer, its remaining grain configuration is sufficiently similar to that of the tubing to identify it as Inconel. A precipitate is present in both the spacer (top of the picture) and in the tubing. Odd transgranular and intergranular cracks or heavy precipitates are discernable in the base tubing.

Figure III-22 shows the extent to which the spacer was transformed from an admittedly large-grained, but fairly normal, material to some completely different appearing alloy. This change was probably caused by some factor in the brazing technique - perhaps time at temperature or selection of braze material. Figure III-23, another portion of the braze zone at higher magnification shows the grain structure which this alloy assumed. The clear white zone at the top of both photos might be weld metal left there when this spacer was reworked. Figure III-24 illustrates the brazed zone at another point on the periphery of this interface. Voids and the peculiar, although characteristic, grain structure are again present.

Photographs taken during the hot cell examination showed cracks or heavy precipitates in the tube wall. Observation of these areas at high magnifications definitely established that cracks did exist, with some boundaries quite widely separated. These cracks were both trans- and inter-granular; the latter were more prevalent. Some were approximately parallel to the tube surface.

It is believed that the observed attack and corrosion resulted from the braze material interacting with the Inconel tubing. It is curious that only one spacer showed such damage while the others appeared to be sound. However, this one may have attained a higher temperature during brazing or during irradiation. Other spacers may have evidenced this same attack, but to an extent not noticeable.

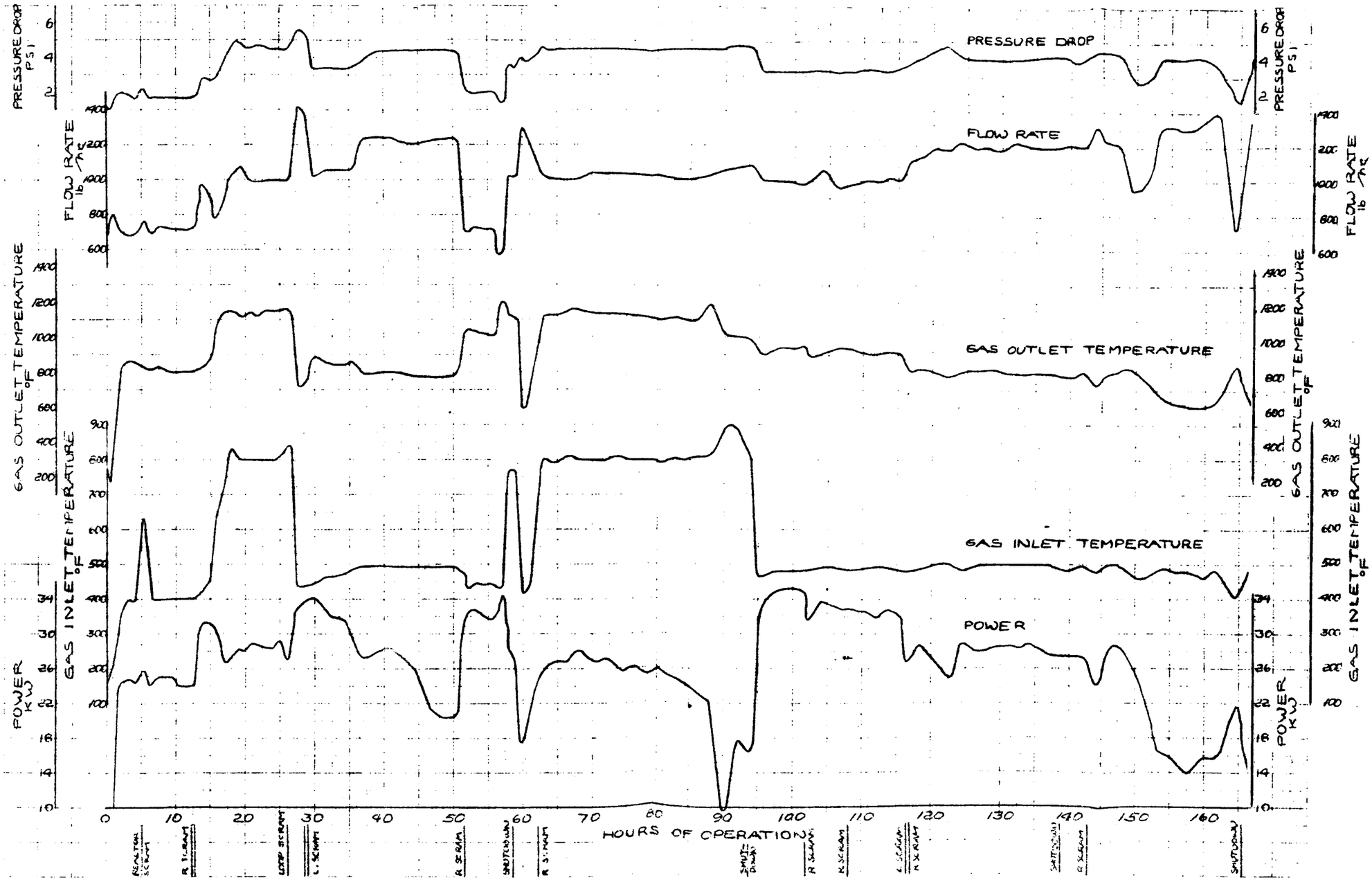

Figure III-1 : IB-1CT OPERATING HISTORY

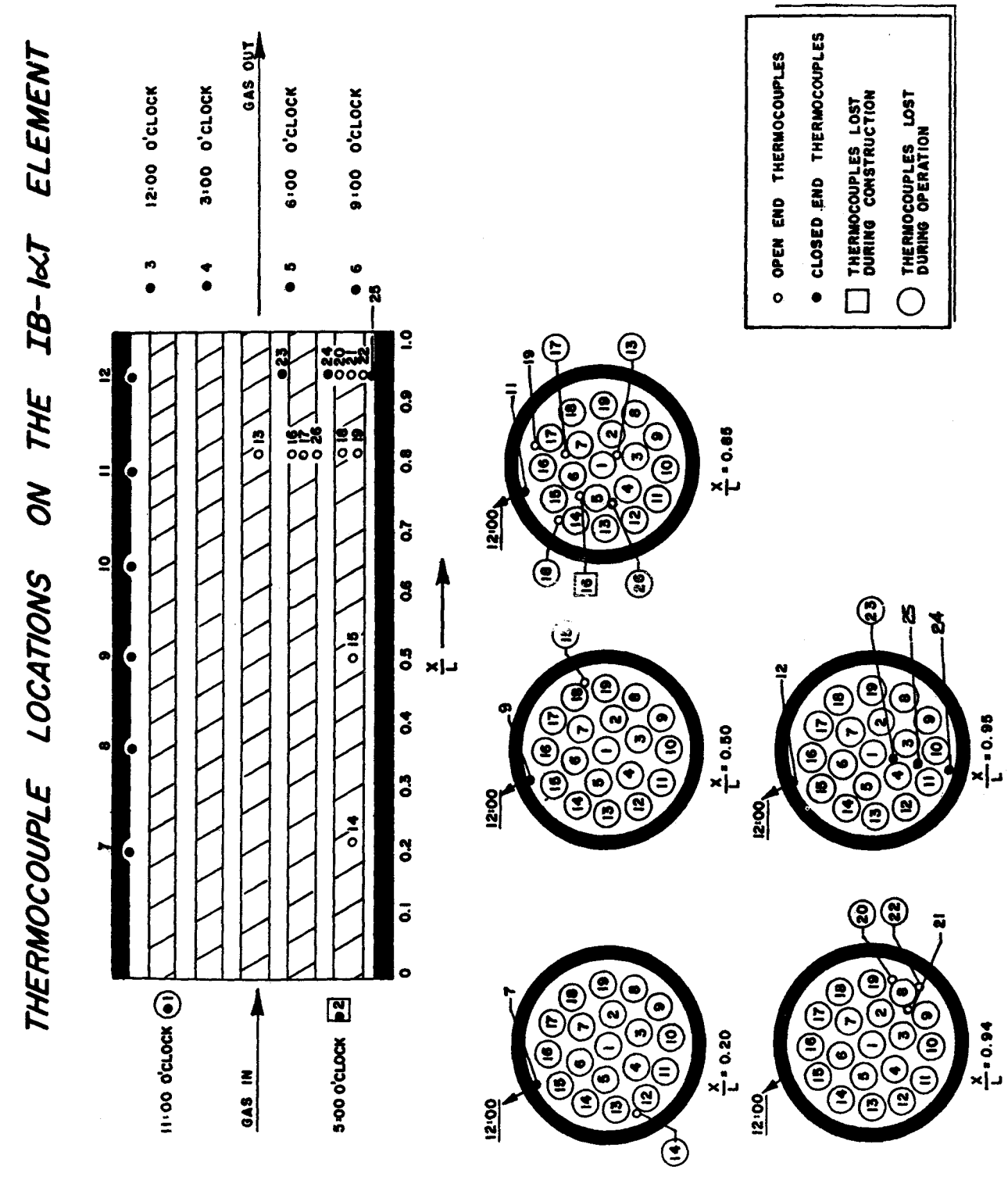
THERMOCOUPLE LOCATIONS ON THE IB-IcT ELEMENT
12:00 O'CLOCK
3:00 O'CLOCK
6:00 O'CLOCK
9:00 O'CLOCK
GAS OUT
11:00 O'CLOCK
GAS IN
5:00 O'CLOCK
OPEN END THERMOCOUPLES
CLOSED END THERMOCOUPLES
THERMOCOUPLES LOST DURING CONSTRUCTION
THERMOCOUPLES LOST DURING OPERATION

Figure III-2

Figure III-3

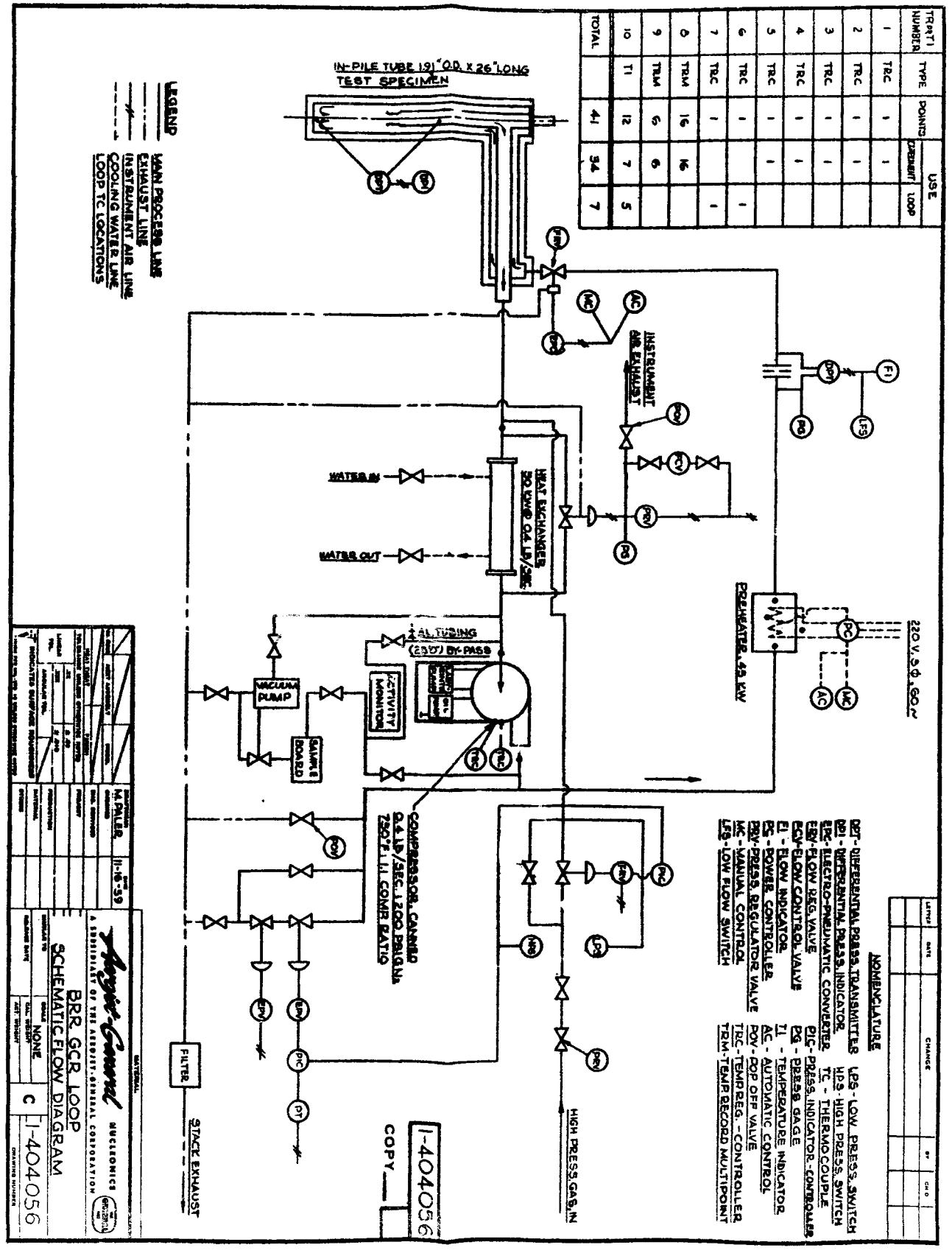
TRAT'I NUMBER
TYPE
POINTS
USE
EXPERIMENT
LOOP
TOTAL
TRC
TRM
TI
IN-PILE TUBE 1.91" O.D. X 26" LONG TEST SPECIMEN
LEGEND
MAIN PROCESS LINE
EXHAUST LINE
INSTRUMENT AIR LINE
COOLING WATER LINE
LOOP TC LOCATIONS
NOMENCLATURE
DPT - DIFFERENTIAL PRESS. TRANSMITTER
DPI - DIFFERENTIAL PRESS. INDICATOR
EPC - ELECTRO-PNEUMATIC CONVERTER
EBV - FLOW REG. VALVE
FCV - FLOW CONTROL VALVE
FI - FLOW INDICATOR
FRC - POWER CONTROLLER
PRV - PRESS. REGULATOR VALVE
MC - MANUAL CONTROL
LFS - LOW FLOW SWITCH
LPS - LOW PRESS. SWITCH
HPS - HIGH PRESS. SWITCH
TC - THERMOCOUPLE
PIC - PRESS. INDICATOR-CONTROLLER
PGS - PRESS. GAGE
TI - TEMPERATURE INDICATOR
AIC - AUTOMATIC CONTROL
POV - POP OFF VALVE
TRC - TEMP. REG. - CONTROLLER
TRM - TEMP. RECORD MULTIPOINT
220 V. 3 Ø. 60 ~
PREHEATER, 45 KW
WATER IN
WATER OUT
HEAT EXCHANGER 30 KW @ 0.4 LB/SEC
AL. TUBING (230') BY-PASS
ACTIVITY MONITOR
VACUUM PUMP
SAMPLE BOARD
COMPRESSOR, CANNING 0.4 LB/SEC, 1200 PSIG IN 720°F, 1.1:1 COMP. RATIO
FILTER
STACK EXHAUST
HIGH PRESS. GAS IN
I-404056
COPY
Aerojet-General
A SUBSIDIARY OF THE AEROJET-GENERAL CORPORATION
NUCLEONICS
BRR GCR LOOP
SCHEMATIC FLOW DIAGRAM
SIZE C
I-404056
SCALE NONE

IB-1 & T ELEMENT
RANGE OF OPERATING TEMPERATURE

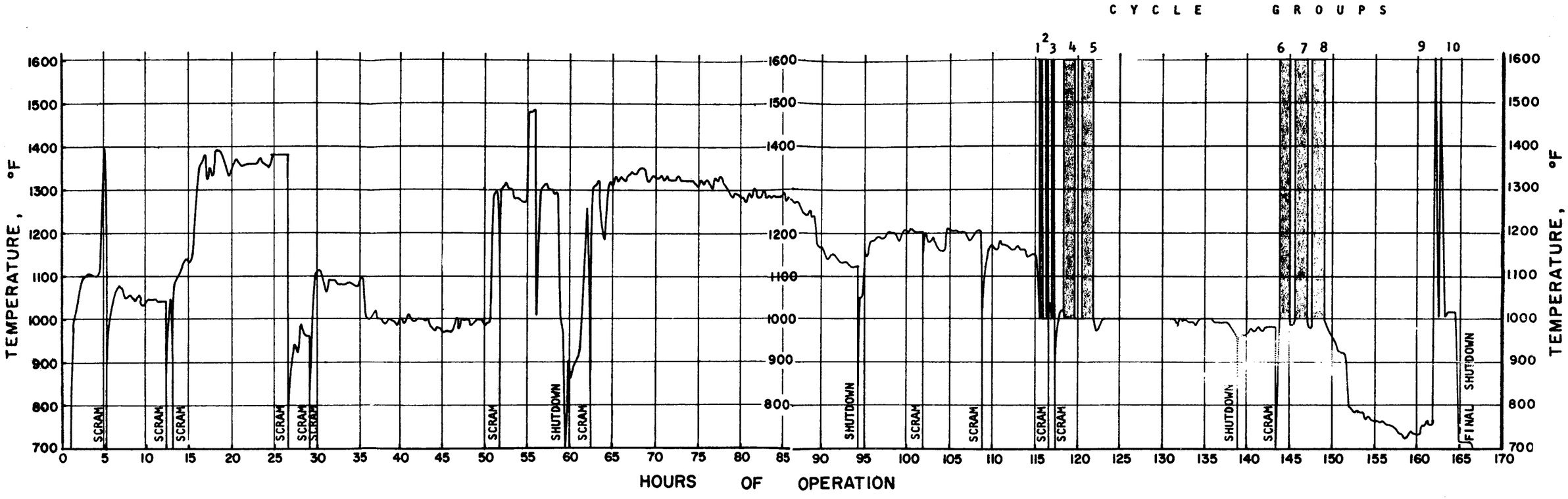

These curves represent an average of the temperatures recorded by Thermocouple #19. There is an oscillation impressed upon these curves with an amplitude of about $\pm 12^{\circ}F$ and a frequency of about 30 cycles per hour.

The darkened sections represent the temperature during the fast thermal cycling period. The cycling was performed between $1000^{\circ}F$ and $1600^{\circ}F$.

Cycle Group	Cycle Rate	Number of Cycles
1	2.5 cycles / 2 min	25
2	1 cycle / 2 min	4
3	"	8
4	"	39
5	"	40
6	"	36
7	"	50
8	"	50
9	1 cycle / 10 min	1
10	1 cycle / 30 min	1

Figure III-4

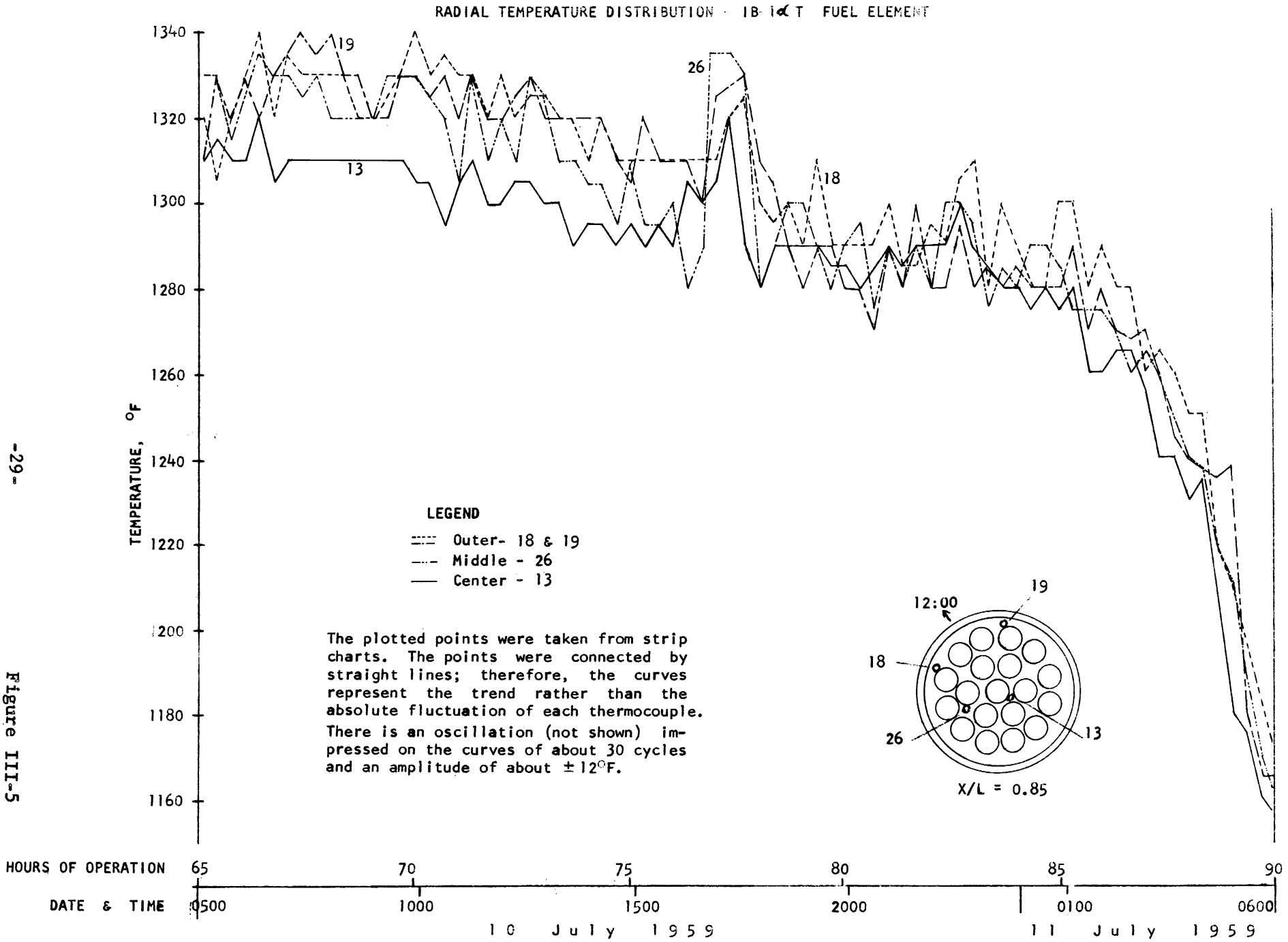
RADIAL TEMPERATURE DISTRIBUTION - IB-1α T FUEL ELEMENT
TEMPERATURE, °F
1340
1320
1300
1280
1260
1240
1220
1200
1180
1160
19
26
18
13
LEGEND
Outer- 18 & 19
Middle - 26
Center - 13
The plotted points were taken from strip charts. The points were connected by straight lines; therefore, the curves represent the trend rather than the absolute fluctuation of each thermocouple. There is an oscillation (not shown) impressed on the curves of about 30 cycles and an amplitude of about ±12°F.
12:00
19
18
26
13
X/L = 0.85
HOURS OF OPERATION
65
70
75
80
85
90
DATE & TIME
0500
1000
1500
2000
0100
0600
10 July 1959
11 July 1959

Figure III-5

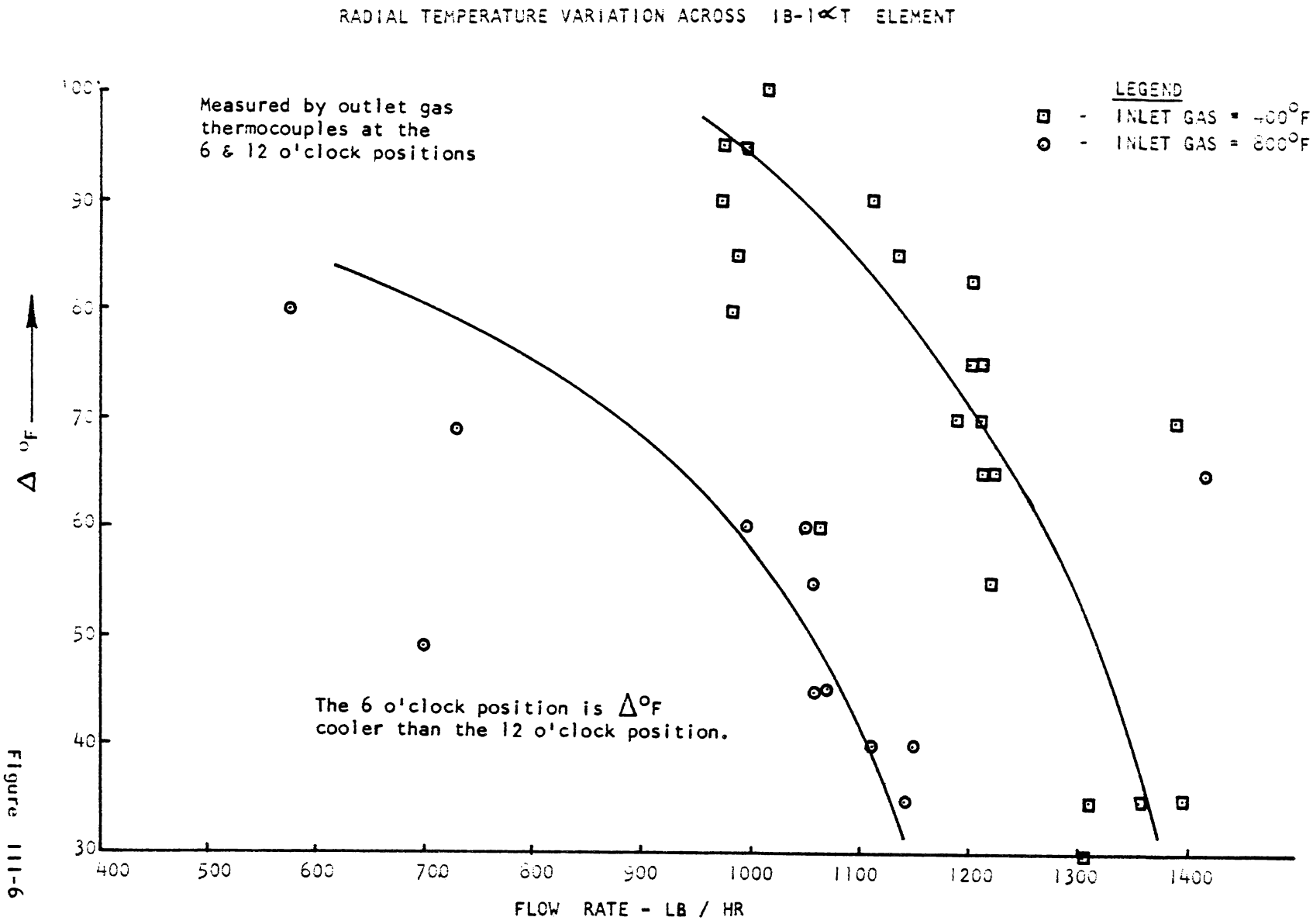
RADIAL TEMPERATURE VARIATION ACROSS IB-1∝T ELEMENT
Measured by outlet gas thermocouples at the 6 & 12 o'clock positions
LEGEND
- INLET GAS = 400°F
- INLET GAS = 800°F
The 6 o'clock position is Δ°F cooler than the 12 o'clock position.
Δ °F
100
90
80
70
60
50
40
30
400
500
600
700
800
900
1000
1100
1200
1300
1400
FLOW RATE - LB / HR

Figure III-6

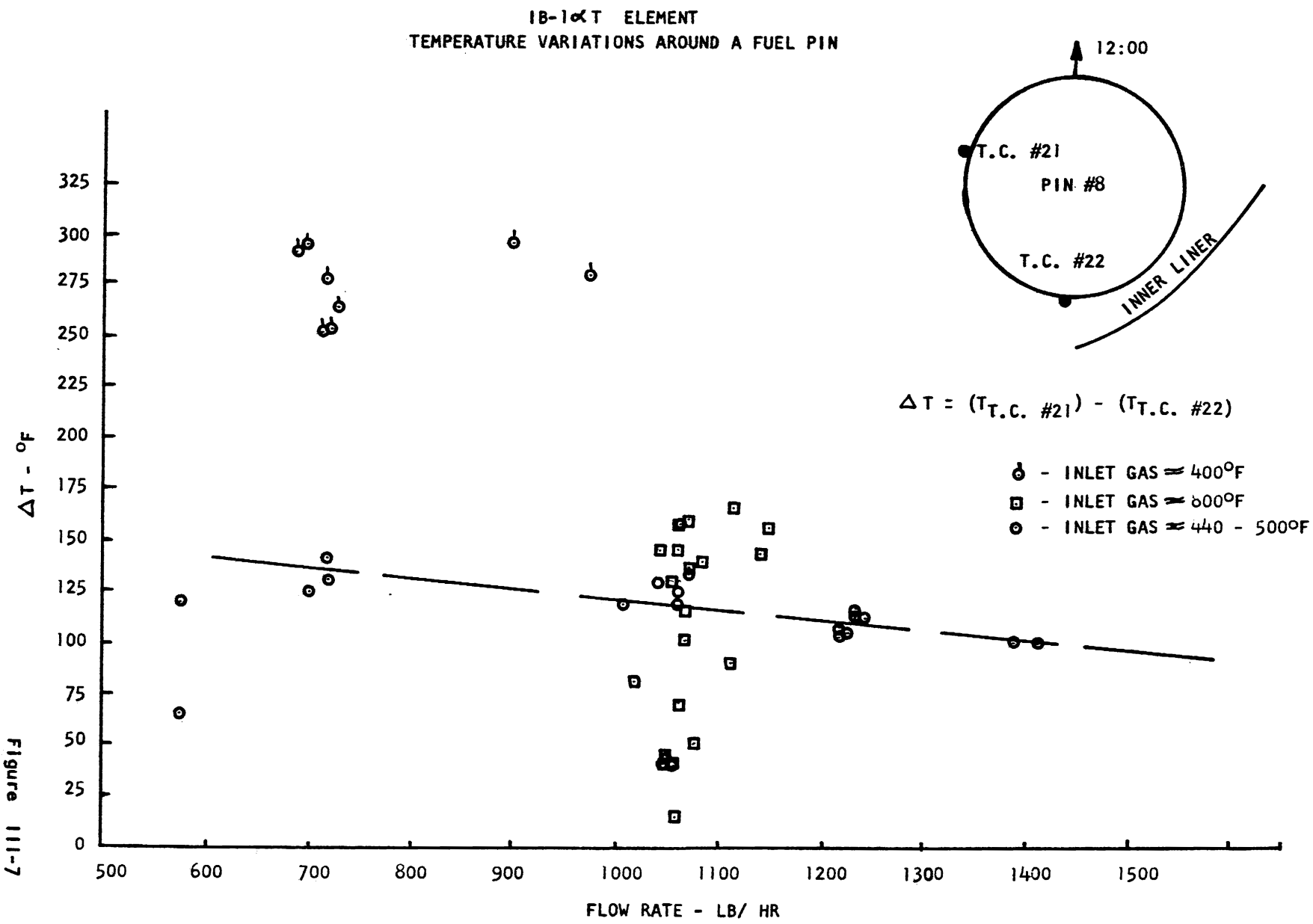
IB-1∝T ELEMENT
TEMPERATURE VARIATIONS AROUND A FUEL PIN
12:00
T.C. #21
PIN #8
T.C. #22
INNER LINER
ΔT = (T T.C. #21) - (T T.C. #22)
- INLET GAS ≈ 400°F
- INLET GAS ≈ 600°F
- INLET GAS ≈ 440 - 500°F
ΔT - °F
0
25
50
75
100
125
150
175
200
225
250
275
300
325
500
600
700
800
900
1000
1100
1200
1300
1400
1500
FLOW RATE - LB/ HR

Figure III-7

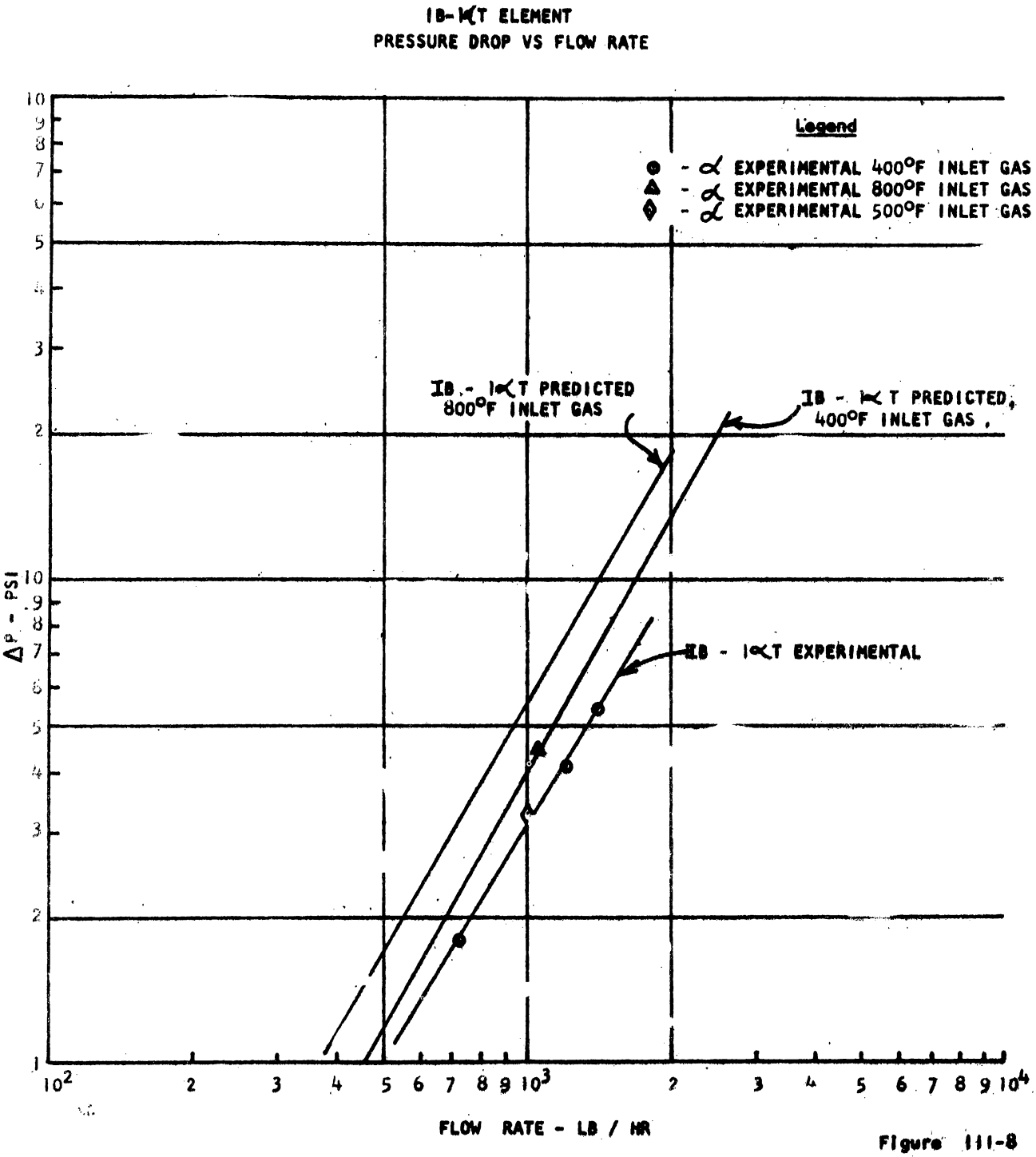
IB-1∝T ELEMENT
PRESSURE DROP VS FLOW RATE
Legend
● - ∝ EXPERIMENTAL 400°F INLET GAS
▲ - ∝ EXPERIMENTAL 800°F INLET GAS
◆ - ∝ EXPERIMENTAL 500°F INLET GAS
IB - 1∝T PREDICTED 800°F INLET GAS
IB - 1∝T PREDICTED, 400°F INLET GAS
IB - 1∝T EXPERIMENTAL
ΔP - PSI
FLOW RATE - LB / HR

Figure III-8

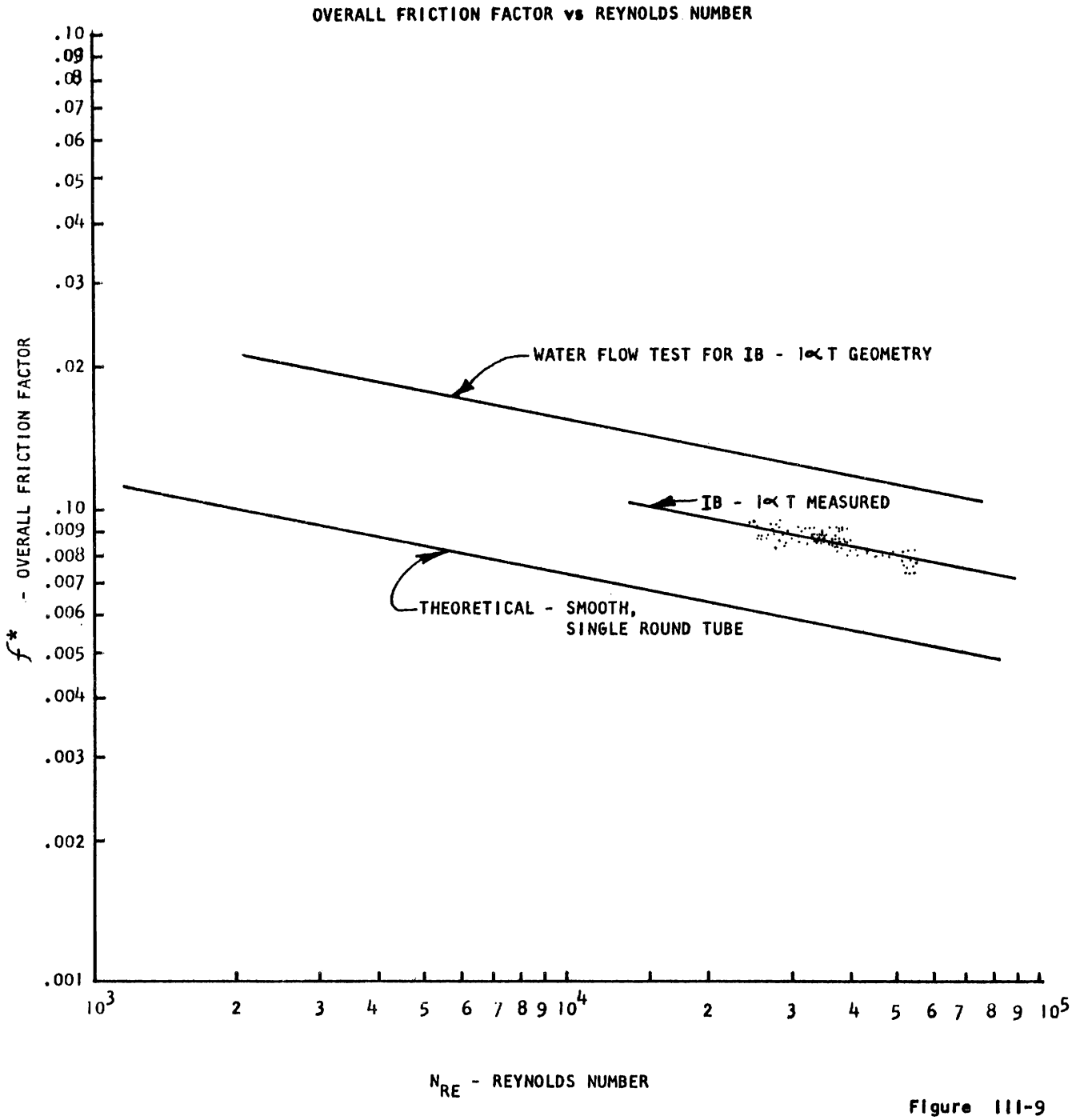
OVERALL FRICTION FACTOR vs REYNOLDS NUMBER
f* - OVERALL FRICTION FACTOR
.10
.09
.08
.07
.06
.05
.04
.03
.02
.10
.009
.008
.007
.006
.005
.004
.003
.002
.001
WATER FLOW TEST FOR IB - I∝T GEOMETRY
IB - I∝T MEASURED
THEORETICAL - SMOOTH,
SINGLE ROUND TUBE
10^3 2 3 4 5 6 7 8 9 10^4 2 3 4 5 6 7 8 9 10^5
N_RE - REYNOLDS NUMBER

Figure III-9

TYPICAL FAST THERMAL CYCLES (1 CYCLE / 2 MINUTES) - IB-1 CT FUEL ELEMENT

Thermocouple #19, X/L = 0.80, Location on Outer Ring

No. 1 Recorder

July 16, 1959

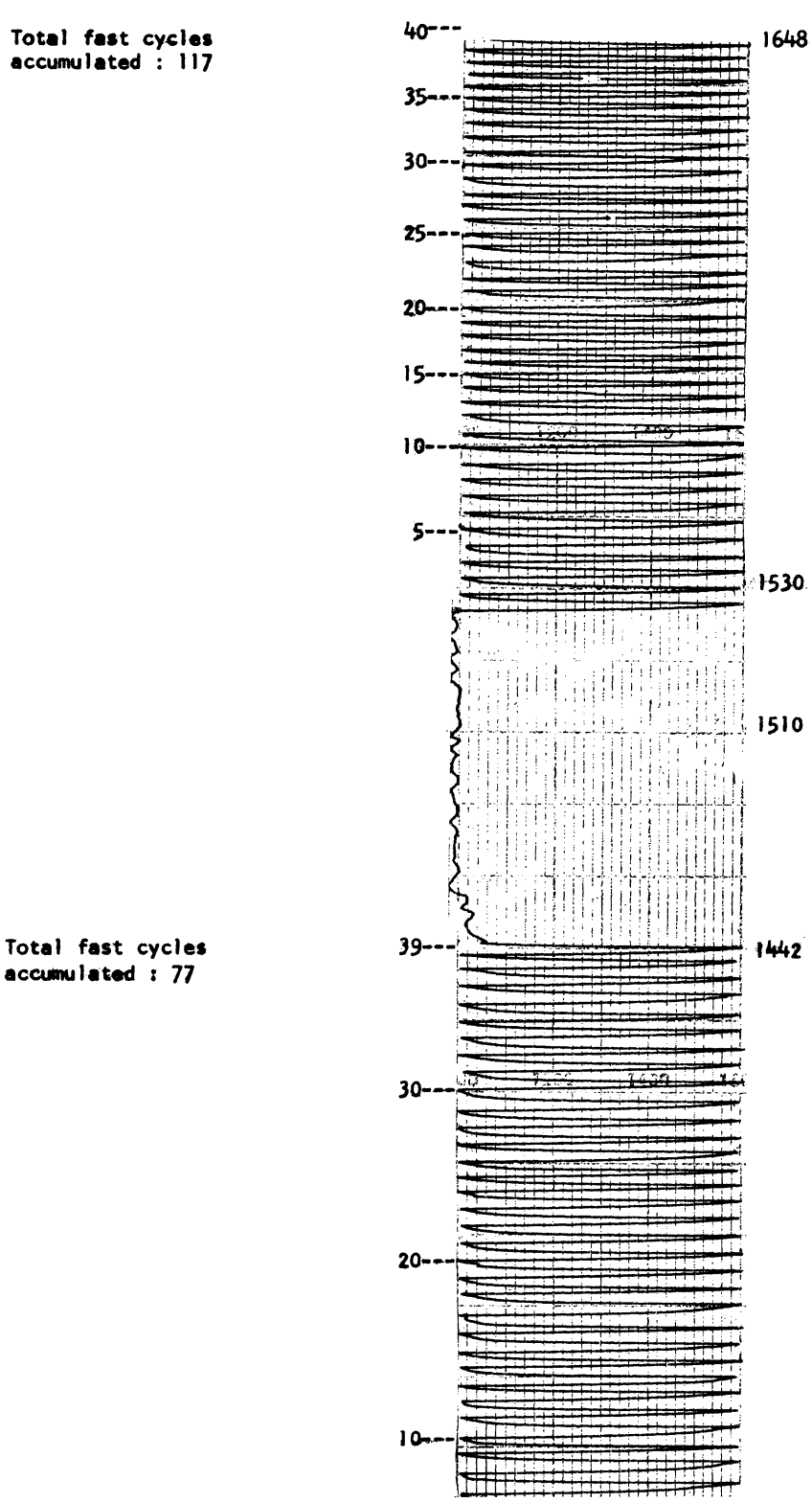

Figure III-10

GAP MEASUREMENTS ON IB-LCT ELEMENT

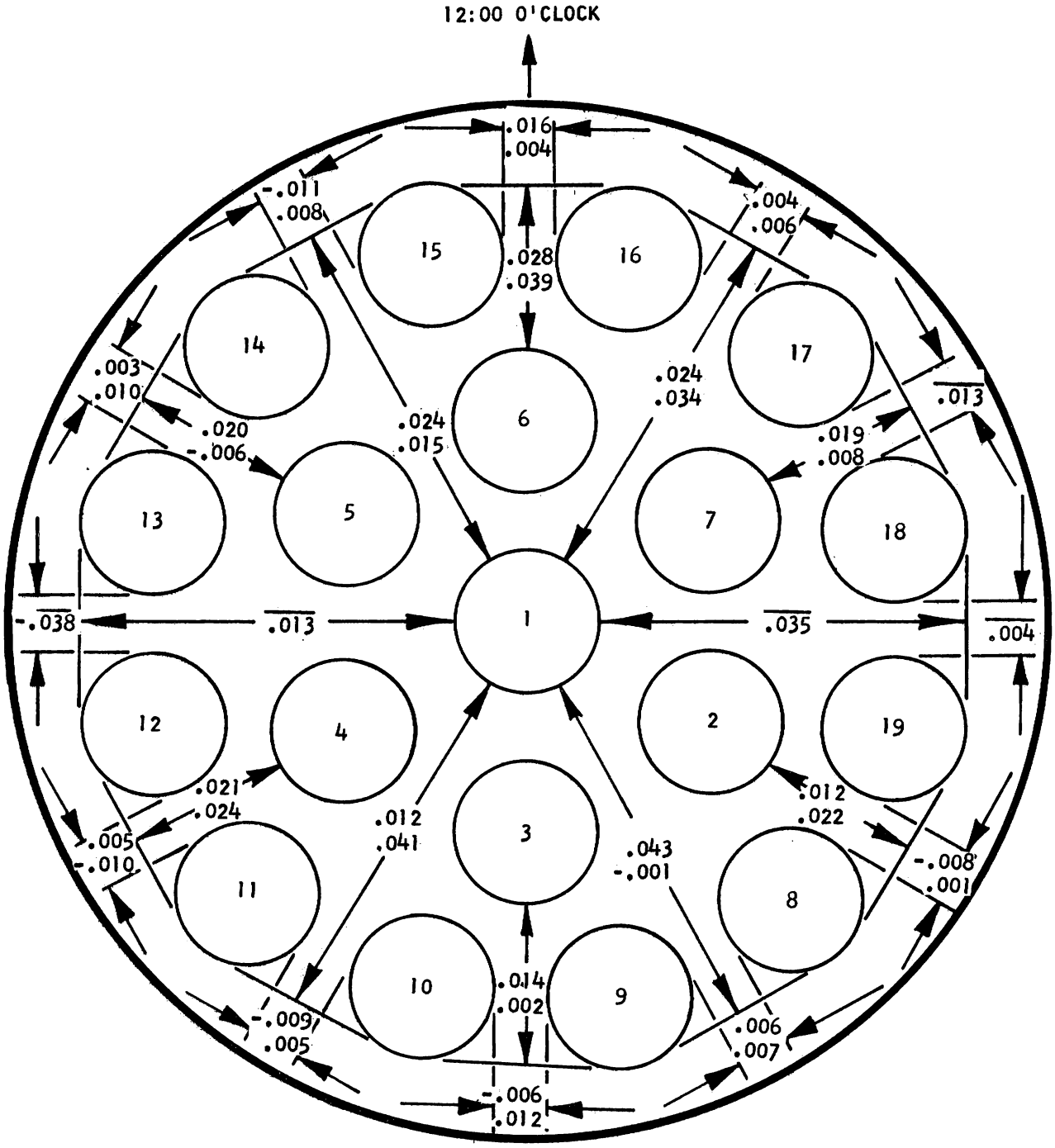

LEGEND

UPPER NUMBER - @ X/L=0.8
LOWER NUMBER - @ X/L=0.5
POSITIVE NUMBER - INCREASE IN GAP
NEGATIVE NUMBER - DECREASE IN GAP
——— - NO MEASUREMENT TAKEN

Figure III-11

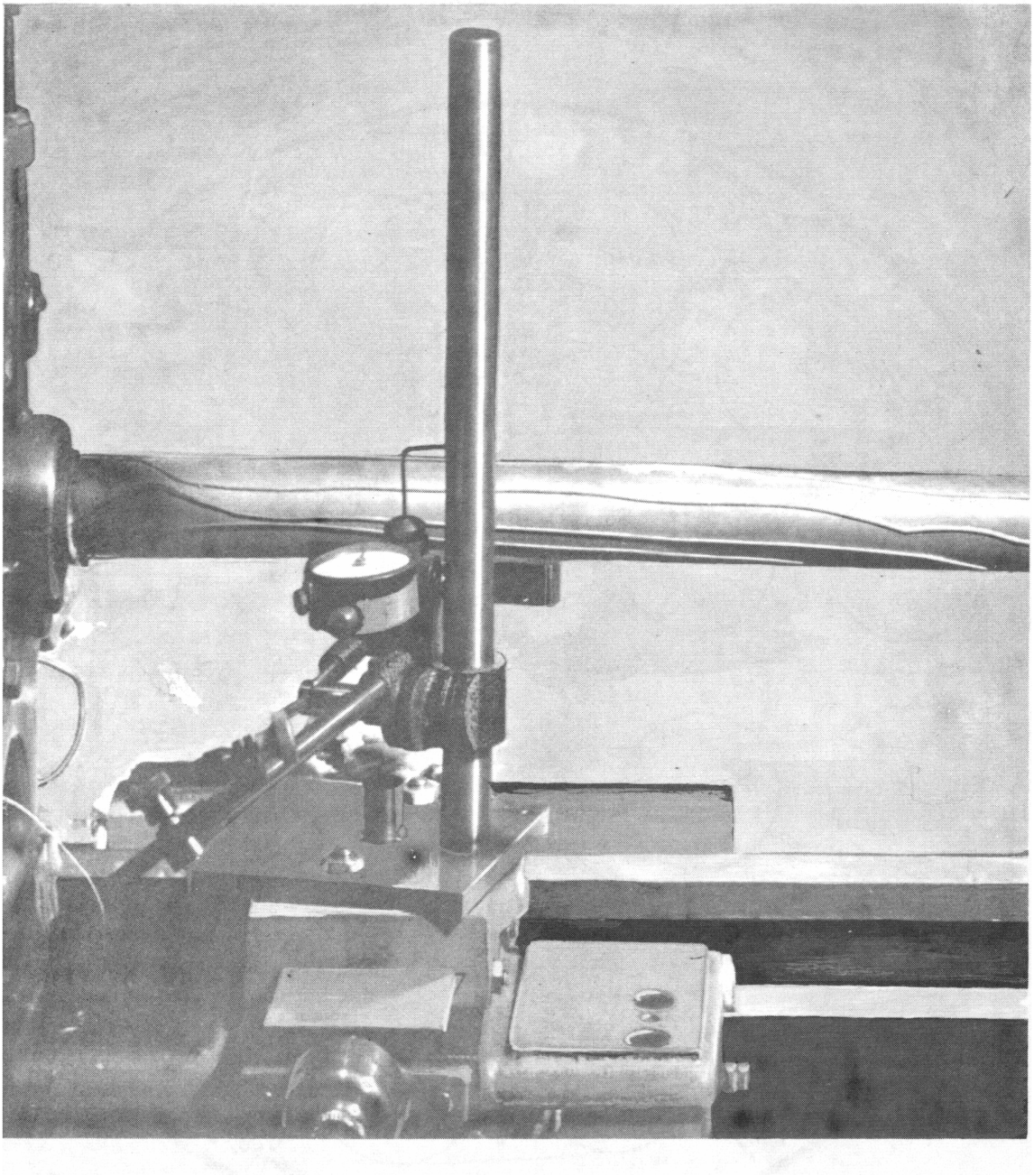

Gap Measuring Gauge

Figure III-12

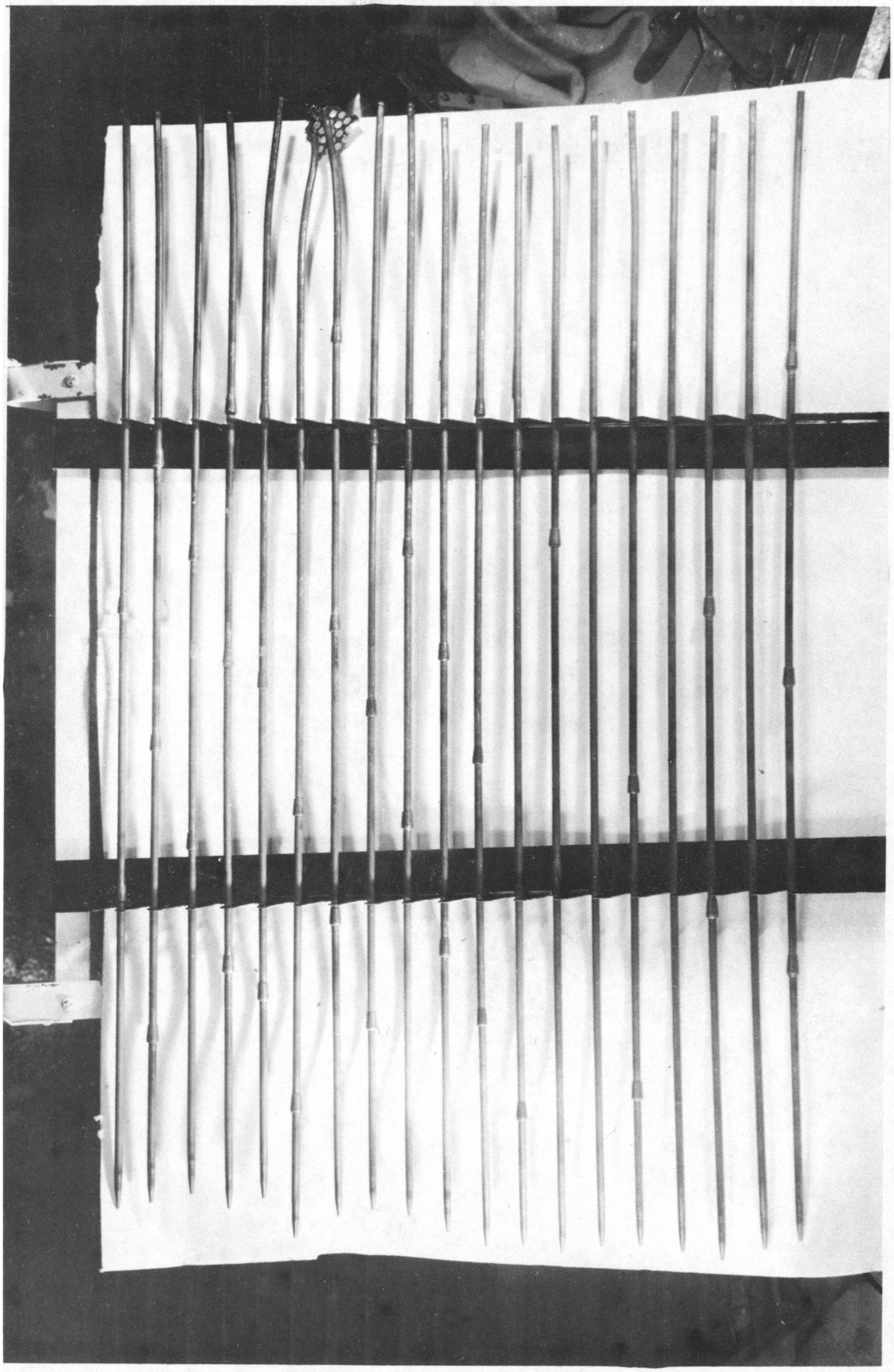

IB-1CT Fuel Pins in Rack

Figure III-13

Figure III-14

Corroded spacer on Pin 16,
IB-1 T element

magnification - 4 x

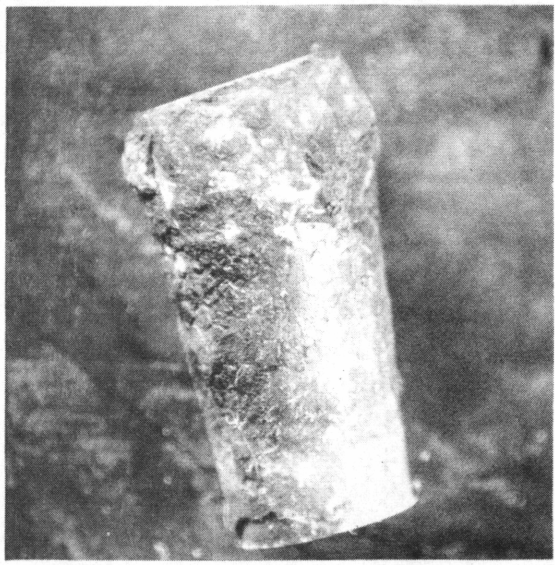

Figure III-15

Corroded spacer after sectioning
magnification - 4 x

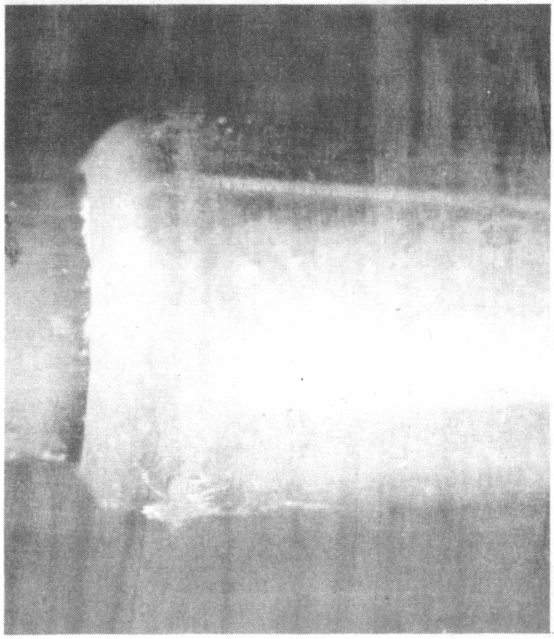

Figure III-16

Typical uncorroded spacer on
IB-1 T element

magnification - 6 x

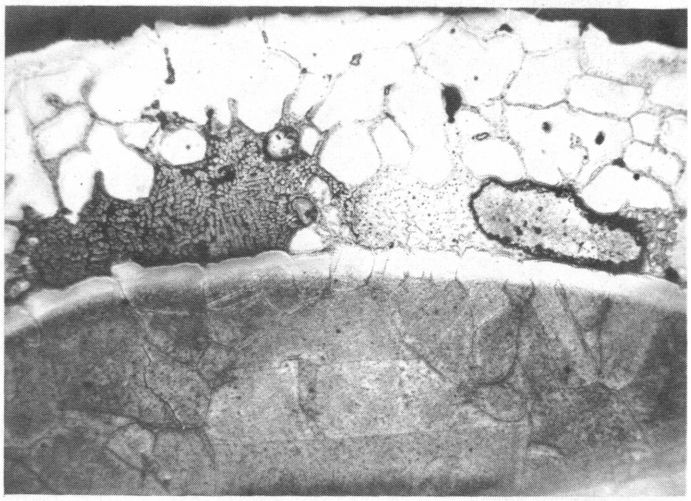

Figure III-17

Section through front end of uncorroded spacer

magnification - 50 x
etchant - 10% oxalic

Figure III-18

Section adjacent to that shown above in Figure III-17.

magnification - 50 x
etchant - 10% oxalic

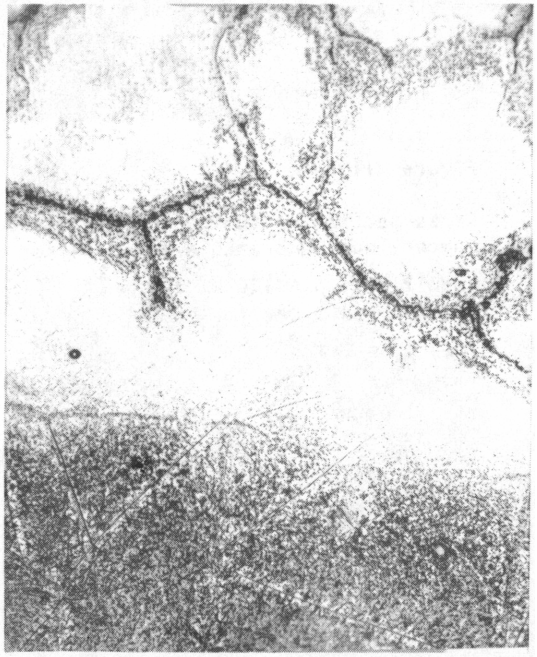

Figure III-19

Corroded spacer and tubing

magnification - 250 x
etchant - 10% oxalic

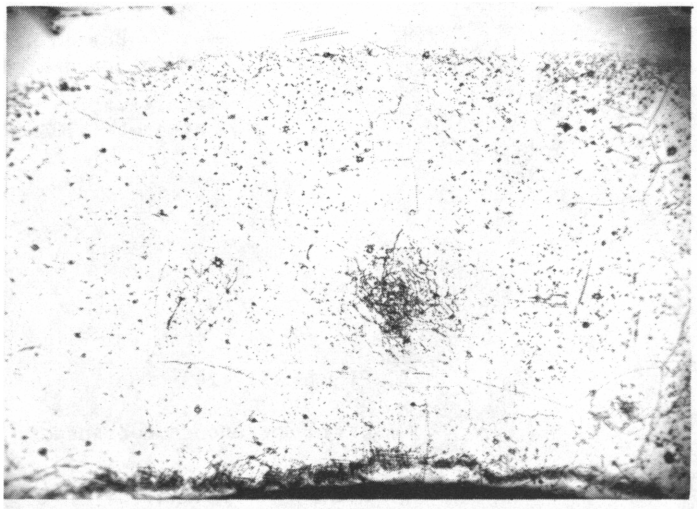

Figure III-20

Cross-section of tubing and uncorroded spacer

magnification - 100 x
etchant - 10% oxalic

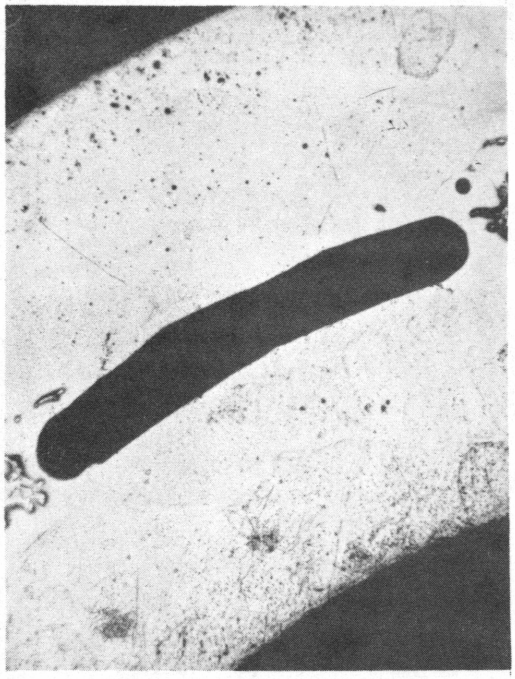

Figure III-21

Cross-section of tubing and uncorroded spacer; note unbrazed area in center

magnification - 100 x
etchant - 10% oxalic

Figure III-22

Cross-section of braze under uncorroded spacer
magnification - 50 x
etchant - 10% oxalic

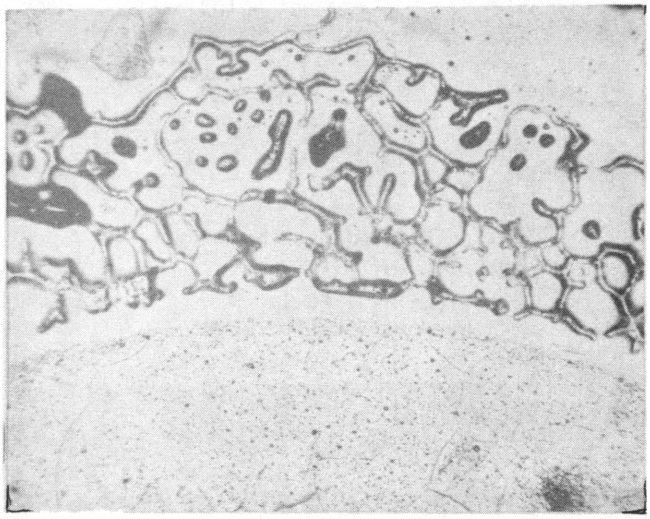

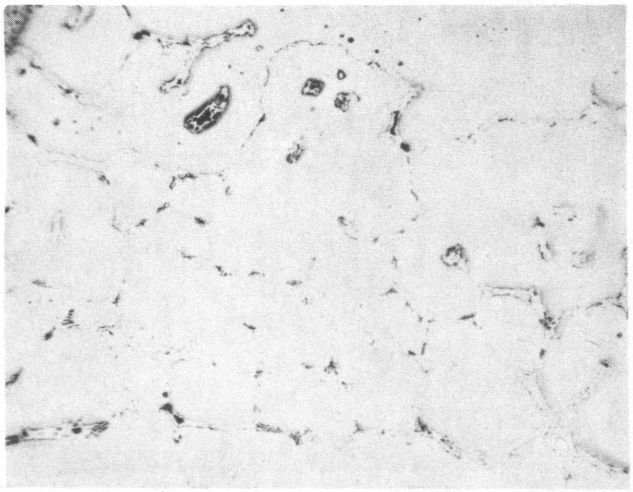

Figure III-23

Brazed section of uncorroded spacer

magnification - 100 x
etchant - 10% oxalic

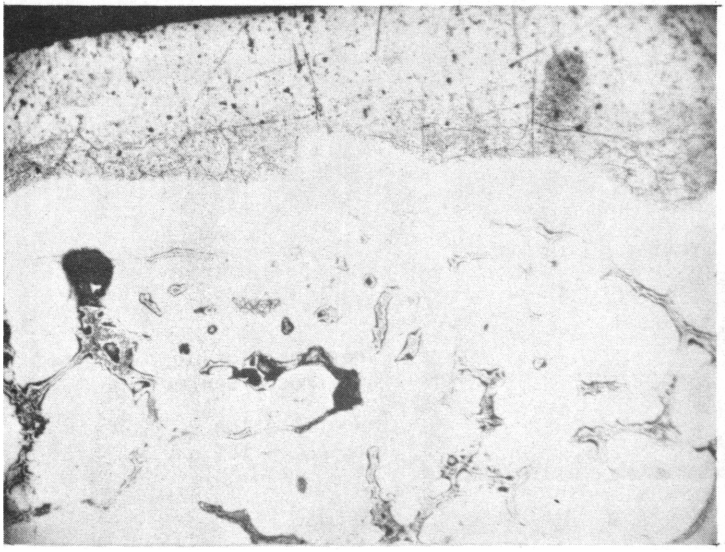

Figure III-24

Braze and uncorroded spacer

magnification - 100 x
etchant - 10% oxalic

IV. THE IB-1/βT TEST

The IB-1/βT was irradiated for a total of 35 hours between 9 September 1959 and 22 September 1959. Post-irradiation studies began in the hot cell on 26 October 1959.

The proposed operating schedule called for establishing steady-state conditions at pin surface temperatures of 1000°, 1200°, 1400°, 1500°, and 1600°F, with the inlet gas at 800°F. Then the element was to be thermally cycled 1000 times, while the fuel pin temperature varied between 1600° and 1000°F at a rate of 10°F/sec. The test was interrupted when a high level of radioactivity was detected in the loop. To determine if the activity was caused by fission gases escaping from the element, a slow thermal cycle was initiated to allow the element to "breath" some fission gas into the loop. The loop activity did increase, and the experiment had to be terminated.

A. INSTRUMENTATION

The IB-1/βT element was instrumented with 34 open-end, closed-end and disc-type thermocouples. Their relative positions in the element are shown in Figure IV-1. True axial locations are listed in Table IV-1 on the following page.

The thermocouples were fabricated of chromel-alumel wire, sheathed in Type-316 stainless steel, and insulated with MgO. The wire diameter was 0.005 in.; the sheath diameter was 0.040 in.

Eleven disc-type junctions were used, for the first time, in an effort to measure the wall temperature of the fuel pin without causing a perturbation in the flow channel. The thermocouple, shown in Figure IV-2, consisted of a circular stainless steel disc (Type-316) 0.020 in. thick. A 0.005-in.-deep hole was machined in the center of the disc. Then the disc was spot-welded to a closed-end thermocouple. The disc was then swaged into a fuel pin at a predetermined axial location. This arrangement placed the sensing point of the disc in the center of the fuel pin. To prevent a large amount of heat from flowing to the disc from the fuel pellet, insulating discs (0.020-in.-thick pellets of stabilized zirconium oxide) were placed on each side of the sensing disc to hold the fuel away from the sensing disc. These insulating discs had a thermal conductivity of about 7 Btu-in./hr-sq ft-°F.

TABLE IV-1

POSITION OF THE IB-1βT THERMOCOUPLES

Thermocouple	Temperature Measured	Axial Location on Element X/L	Junction Type
1	Inlet gas	-0.062	Closed-end
3	Outlet gas	1.23	Closed-end
4	Outlet gas	1.23	Closed-end
5	Outlet gas	1.23	Closed-end
6	Outlet gas	1.23	Closed-end
7	Inner liner	0.051	Closed-end
8	Inner liner	0.202	Closed-end
10	Inner liner	0.501	Closed-end
11	Inner liner	0.732	Closed-end
12	Inner liner	0.904	Closed-end
13	Pin wall	0.732	Disc
14	Pin wall	0.052	Disc
15	Pin wall	0.202	Disc
17	Pin wall	0.500	Disc
18	Pin wall	0.732	Disc
19	Pin wall	0.977	Disc
20	Pin wall	0.051	Open-end
22	Pin wall	0.352	Disc
23	Pin wall	0.501	Disc
24	Pin wall	0.732	Disc
25	Pin wall	0.732	Disc
26	Pin wall	0.978	Disc
27	Periphery of pin	0.978	Open-end
28	Periphery of pin	0.978	Open-end
29	Periphery of pin	0.978	Open-end
30	Periphery of pin	0.978	Open-end
32	Periphery of pin	0.978	Open-end
34	Pellet center	0.732	Closed-end

Closed-end thermocouples measured the liner temperatures, gas inlet and exit temperatures, and the temperature at the center of the ceramic fuel. Open-end thermocouples were used on two fuel pins to measure the outside wall temperatures of the pins, and to check the readings of the disc thermocouples. Table IV-2, on the following page, lists the thermocouples that became inoperative during irradiation or construction of the IB-1βT element.

TABLE IV-2

INOPERATIVE IB-1βT THERMOCOUPLES

Thermocouple No.	Location	Type	Axial Location on Element X/L	Length of Operation Hours
2	Gas inlet	Closed-end	below .00	Lost in construction
8	Inner liner	Open-end	.20	0
9	Inner liner	Open-end	.35	Lost in construction
14	Pin No. 2	Disc	.05	2
15	Pin No. 3	Disc	.20	18
16	Pin No. 4	Disc	.35	Lost in construction
21	Pin No. 9	Disc	.20	Lost in construction
24	Pin No. 13	Disc	.73	10
31	Pin No. 16	Open-end	.98	Lost in construction
33	Inside fuel pellet, Pin No. 12	Closed-end	.73	Lost in construction

It was predicted that the disc-type thermocouples would indicate a temperature about 5% of the film drop higher than the true pin wall temperature. The accuracy of this analysis is such that a confidence of about 80% is placed in it.

B. PERFORMANCE CHARACTERISTICS

1. Heat Transfer

The operating temperature range of the IB-1βT is shown in Figure IV-3. This plot shows the temperature at the expected element hot spot (X/L = 0.73).

a. Axial Temperature

The IB-1βT element was instrumented to obtain temperature profiles of the inner liner, and the two rings of fuel pins. These experimental temperature profiles were plotted for 6 different periods of accumulated irradiation, as shown in Table IV-3, on the following page. Two profiles are shown in Figures IV-4 and -5; these were a representation of the experimental temperature profiles after 11.6 and 26.0 hours of irradiation.

TABLE IV-3

IB-1βT EXPERIMENTAL DATA

Duration of Operation (Hours)	Flow Rate (lb/hr)	Gas Inlet Temp. (^{o}F)	Gas Outlet Temp. (^{o}F)	Element Power (kw)	Loop Pressure (psia)
0.3	1135	370	741	31.7	199
9.2	1040	770	1110	27.9	204
11.6*	1010	800	1199	32.2	205
19.4	734	800	1291	2819	200
26.0*	645	800	1352	28.5	205
31.0	583	810	1408	27.9	201

* Data plotted in Figures IV-4 and -5.

b. Circumferential Element Temperature

The IB-1βT also had 4 thermocouples located 6.5 in. above the fuel region. These thermocouples showed that the temperature relationship around the IB-1βT was the same as that around the IB-1αT. The 12 o'clock position was hottest; the 6 o'clock, coolest; and the 3- and 9-o'clock temperatures ranged between these limits (see Figure IV-6). The large difference in the temperatures around the element (80^{o}-150^{o}F) indicates that mixing between flow passages was not complete.

The relationship between the bulk coolant temperature increases of the 12- and 6-o'clock sectors was somewhat different than the relationship found in the IB-1αT. In the IB-1βT element the bulk coolant temperature increase on the 12 o'clock side was 29 to 32% greater than that on the 6 o'clock side, but the increase was independent of flow rate.

The comparison of the temperatures between the rings was made at the point where X/L = 0.73. As was the case in the IB-1αT test, no ring in the IB-1βT element was consistently hotter or cooler than another ring. As shown in Figure IV-3, the center pin was nominally 50^{o}F hotter than the outer ring, and 20^{o} to 40^{o}F hotter than the intermediate ring. During the first 11 hr of operation, changes in ring temperatures occurred after thermal shocks, indicating that the thermocouple calibration changed between thermal cycles.

c. Circumferential Pin Temperature

Two of the IB-1βT fuel pins were instrumented to obtain circumferential temperature variations. Pin 5 (on the intermediate ring) had 3 thermocouples, and Pin 17 (outer ring) had 2 thermocouples spot-welded to its outer surface. All the thermocouples were at the axial position where X/L = 0.978. Pin 5 showed a maximum variation in temperature of 45°F, while Pin 16 had only a 10°F variation around the pin. These thermocouple temperature readings are plotted against flow rate in Figure IV-7.

There is less temperature variation around the IB-1βT fuel pins than around the IB-1αT pins because the IB-1βT thermocouples were located only 0.46 in. below the top of the fuel, while the IB-1αT thermocouples were 1.40 in. below the top of the fuel region. Since the IB-1βT thermocouples had less fuel above them, the heat losses would be greater; heat would be conducted up the thermocouple sheath and pin wall and make the thermocouple temperature approach the gas temperature.

d. Fin Effectiveness

The heat transfer effectiveness of the fins on the IB-1βT element was analyzed by comparing the change in hA (product of average heat transfer coefficient and surface areas) for a finned pin element and a smooth pin element. Heat generated within the pins and transferred to the gas can be expressed as

$$Q = hA \ \Delta T_f,$$

Where

Q = heat generation (Btu/hr)

h = average heat transfer coefficient from outside pin wall to the coolant stream (Btu/hr ft^2°F)

A = heat transfer area (ft^2)

ΔT_f = average temperature difference between the bulk coolant gas and outside fuel pin wall.

Heat transferred to the coolant gas can also be expressed as

$$Q = \dot{W} C_p (T_o - T_i)$$

Where

Q = heat generation rate (Btu/hr)

$\dot{W}$ = coolant mass flow rate (lb/hr)

C_p = heat capacity (Btu/lb °F)

$(T_o - T_i)$ = increase in bulk coolant temperature (°F).

When there is negligible heat loss (from the element through the insulation to the re-entrant gas stream) these heat generation rates are identical and can be equated

$$hA \, \Delta T_f = W \, C_p \, (T_o - T_i)$$

$$hA = \frac{W \, C_p \, (T_o - T_i)}{\Delta T_f}$$

The mass flow rate, inlet temperature, and outlet temperature were directly measured during operation; and the heat capacity could be determined quite accurately from known conditions of pressure and temperature. The average temperature difference between bulk coolant gas and the outside fuel pin wall (ΔT_f) was determined by plotting fuel pin temperature at various points along the length of the pin, with the corresponding bulk gas temperature, and obtaining the average difference between these temperatures (see Figures IV-8 and -9).

The comparison of finned and smooth pins indicated that the addition of longitudinal fins to the fuel pins increased hA by about 10%. This analysis was quite rough, and the apparent increase in heat transfer obtained with the use of fins is within the uncertainty envelope.

2. Fluid Flow

The instrumentation used to measure fluid flow was identical to that used in the IB-1αT experiment, and the same discussion of pressure drop applies to the IB-1βT.

The predicted pressure drop of the IB-1βT was 20 to 30% greater than that measured (see Figure IV-10).

C. COOLANT GAS ANALYSIS

The loop gas was analyzed at regular intervals during the IB-1βT experiment. Samples were scanned over the energy range of 0 to 3.0 Mev, using a 100-channel gamma-ray spectrometer.

At the start of irradiation, the loop gas activity was near background. After about 14 hr of operation, the activity increased rapidly from 5 to 42 millicuries, at the 17th hour.

After 17 hr of operation the loop was shut down for about 60 hr, and the activity decreased to 9 millicuries. During the period from about the 17th to 32nd hr of irradiation, the activity fluctuated between 9 and 14 millicuries. The element was cycled thermally (1 cycle in 30 minutes) to see what effect fuel pin "breathing" would have on the loop gas activity. This slow thermal cycle produced a rise in the activity level to 150 millicuries. The major isotopes found in the

gas samples were Xe-133, Xe-135, and Kr-85, the same isotopes identified in the gas samples taken during the IB-1αT experiment. This high level of activity made it necessary to stop the IB-1βT experiment after only 35 hr of irradiation.

D. POST-IRRADIATION EVALUATION

The element did not receive extensive hot cell work because of the short irradiation time. Figure IV-11 shows the IB-1βT pins after separation from the upper pin support. The pins are arranged in order with Pin 1 at the bottom. No distortion of the pins was observed.

Leak-checking was performed in the same manner as with the IB-1αT element. Pins 16 and 2 leaked at the top plug of the fuel pin. These leaks occurred at the point where the sheathed thermocouple was brazed into the top plug.

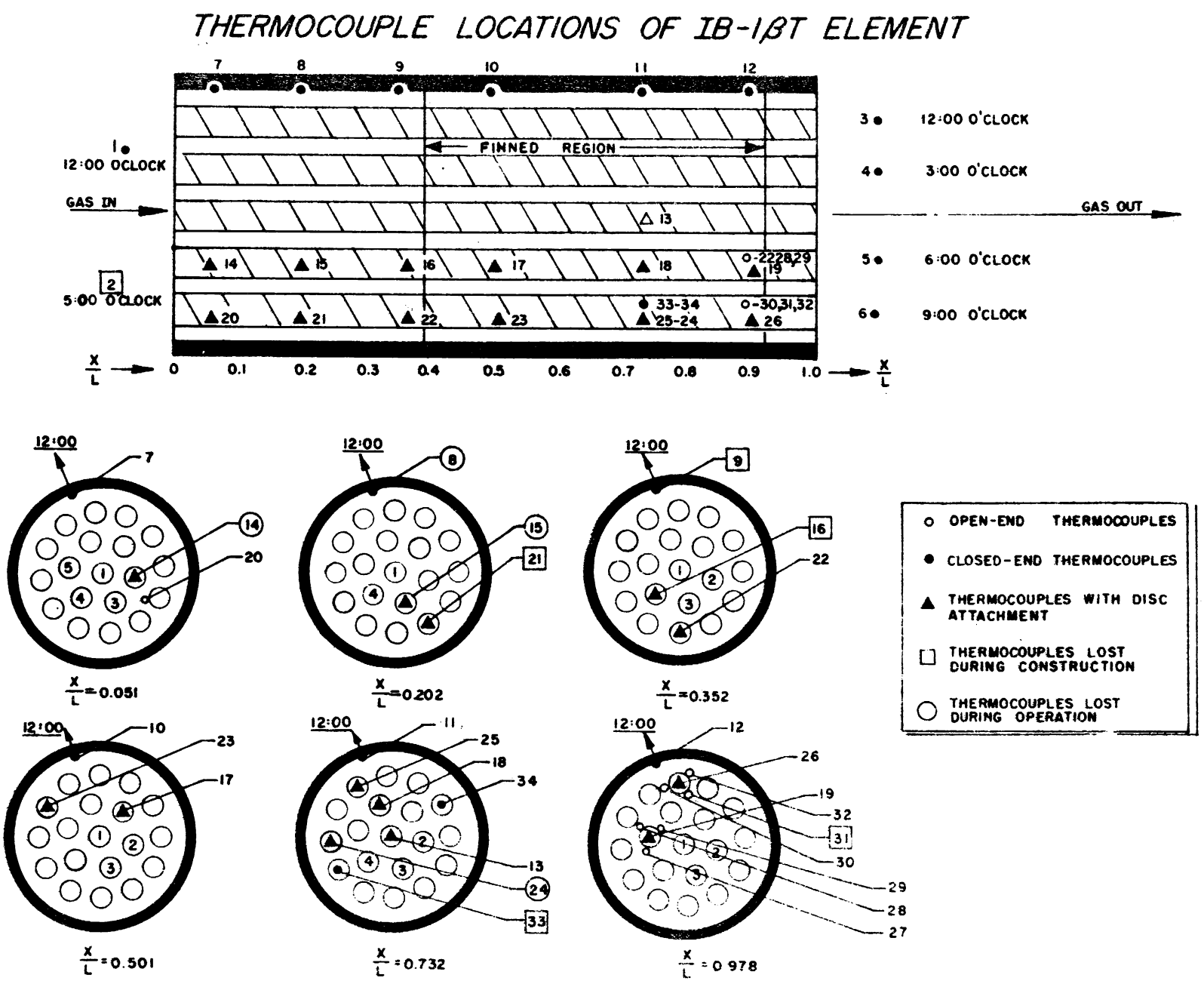
THERMOCOUPLE LOCATIONS OF IB-1βT ELEMENT
7
8
9
10
11
12
1 ● 12:00 OCLOCK
GAS IN
FINNED REGION
3 ● 12:00 O'CLOCK
4 ● 3:00 O'CLOCK
GAS OUT
△ 13
▲ 14
▲ 15
▲ 16
▲ 17
▲ 18
o-22,28,29 ▲ 19
2 5:00 O'CLOCK
5 ● 6:00 O'CLOCK
▲ 20
▲ 21
▲ 22
▲ 23
● 33-34 ▲ 25-24
o-30,31,32 ▲ 26
6 ● 9:00 O'CLOCK
X/L → 0 0.1 0.2 0.3 0.4 0.5 0.6 0.7 0.8 0.9 1.0 → X/L
12:00
7
14
20
5
1
4
3
X/L=0.051
12:00
8
15
21
1
4
X/L=0.202
12:00
9
16
22
1
2
3
X/L=0.352
12:00
10
23
17
1
2
3
X/L=0.501
12:00
11
25
18
34
2
4
3
13
24
33
X/L=0.732
12:00
12
26
19
32
31
30
29
28
27
1
2
3
X/L=0.978
o OPEN-END THERMOCOUPLES
● CLOSED-END THERMOCOUPLES
▲ THERMOCOUPLES WITH DISC ATTACHMENT
□ THERMOCOUPLES LOST DURING CONSTRUCTION
○ THERMOCOUPLES LOST DURING OPERATION

Figure IV-1

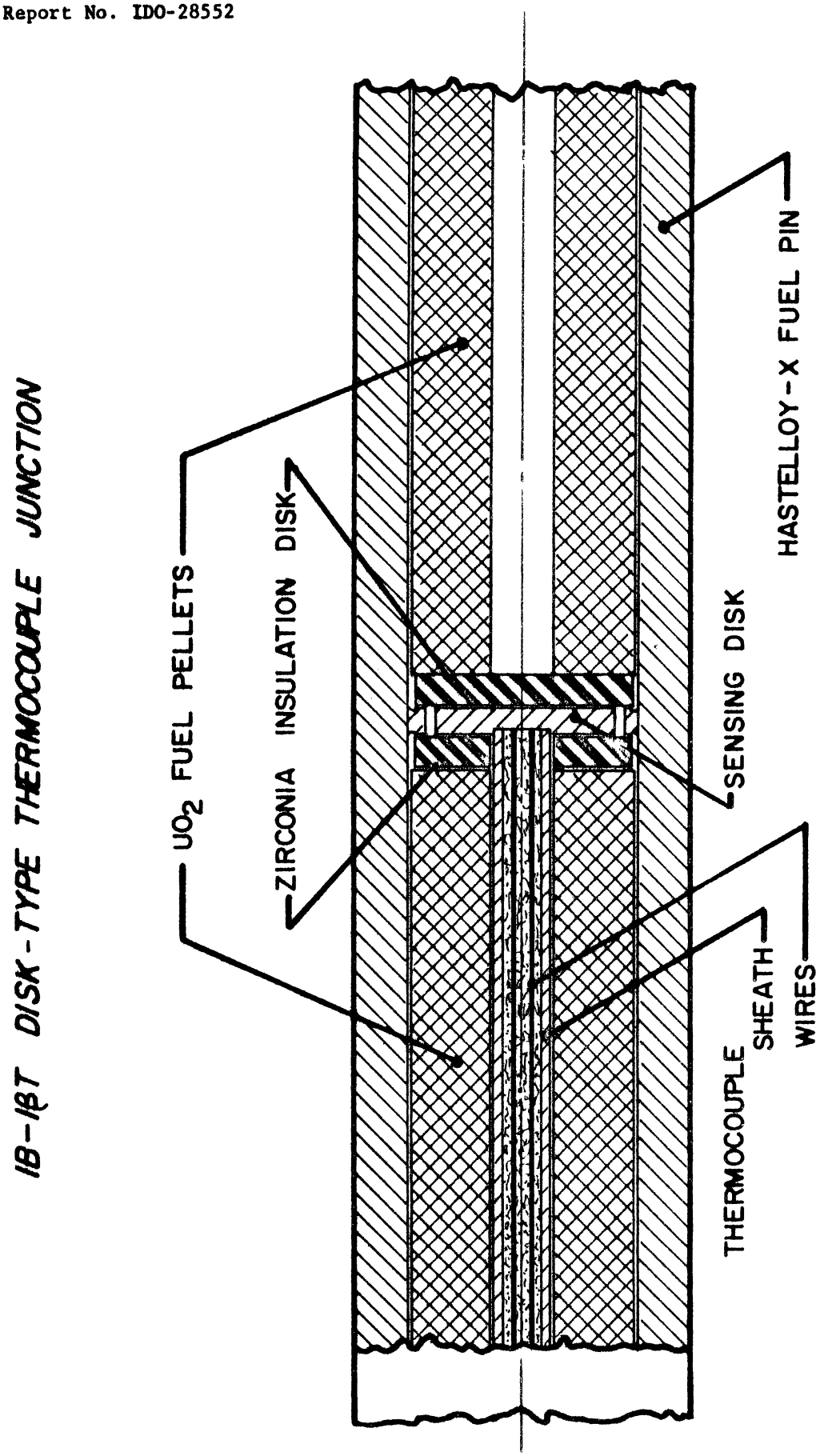
IB-IBT DISK-TYPE THERMOCOUPLE JUNCTION
UO_2 FUEL PELLETS
ZIRCONIA INSULATION DISK
SENSING DISK
HASTELLOY-X FUEL PIN
THERMOCOUPLE
SHEATH
WIRES

Figure IV-2

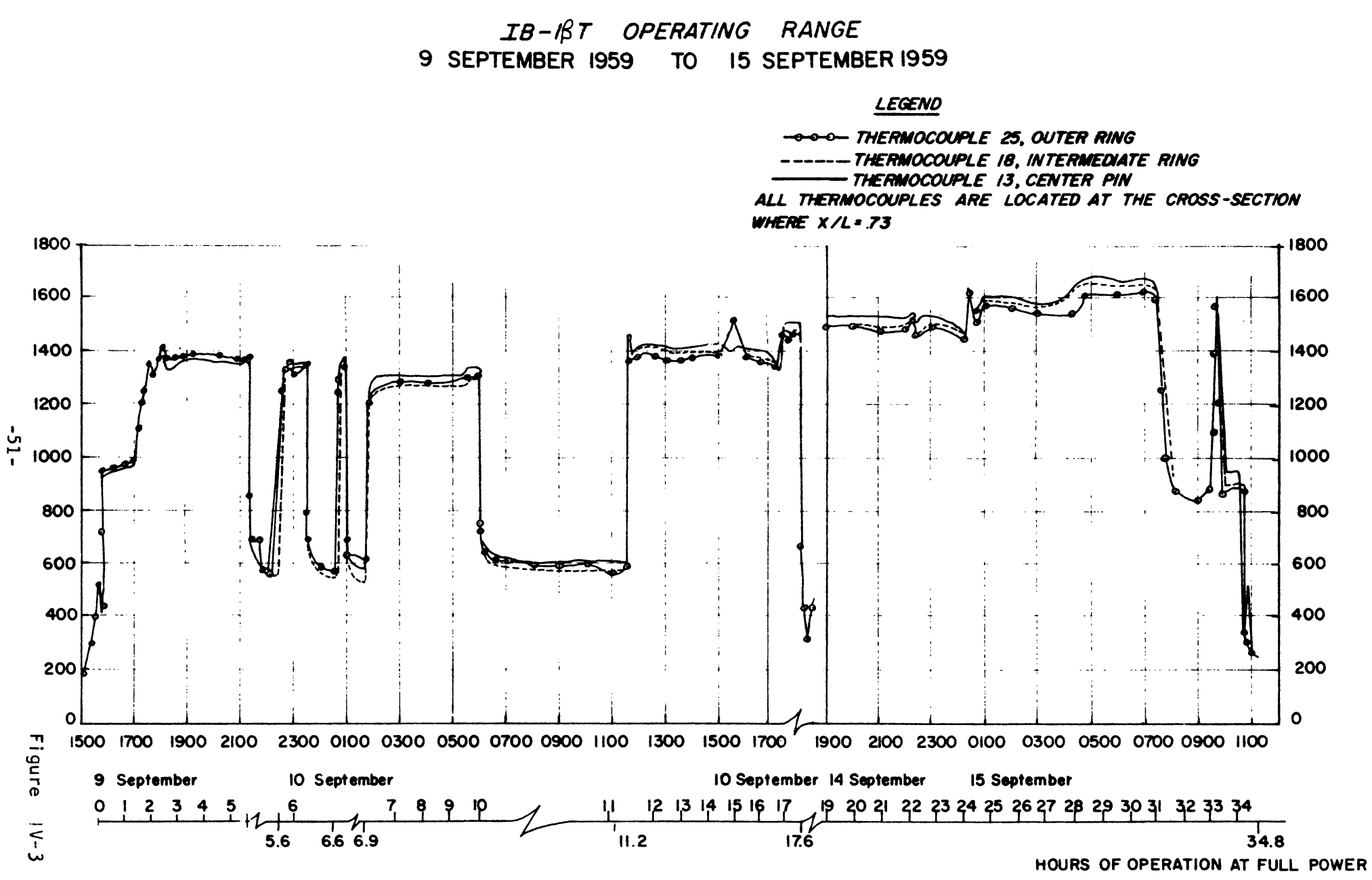
IB-1βT OPERATING RANGE
9 SEPTEMBER 1959 TO 15 SEPTEMBER 1959
LEGEND
THERMOCOUPLE 25, OUTER RING
THERMOCOUPLE 18, INTERMEDIATE RING
THERMOCOUPLE 13, CENTER PIN
ALL THERMOCOUPLES ARE LOCATED AT THE CROSS-SECTION WHERE X/L = .73
1800
1600
1400
1200
1000
800
600
400
200
0
1500 1700 1900 2100 2300 0100 0300 0500 0700 0900 1100 1300 1500 1700 1900 2100 2300 0100 0300 0500 0700 0900 1100
9 September
10 September
10 September
14 September
15 September
0 1 2 3 4 5 6 7 8 9 10 11 12 13 14 15 16 17 19 20 21 22 23 24 25 26 27 28 29 30 31 32 33 34
5.6 6.6 6.9 11.2 17.6 34.8
HOURS OF OPERATION AT FULL POWER

Figure IV-3

TEMPERATURE PROFILE
IB-1/β T ELEMENT

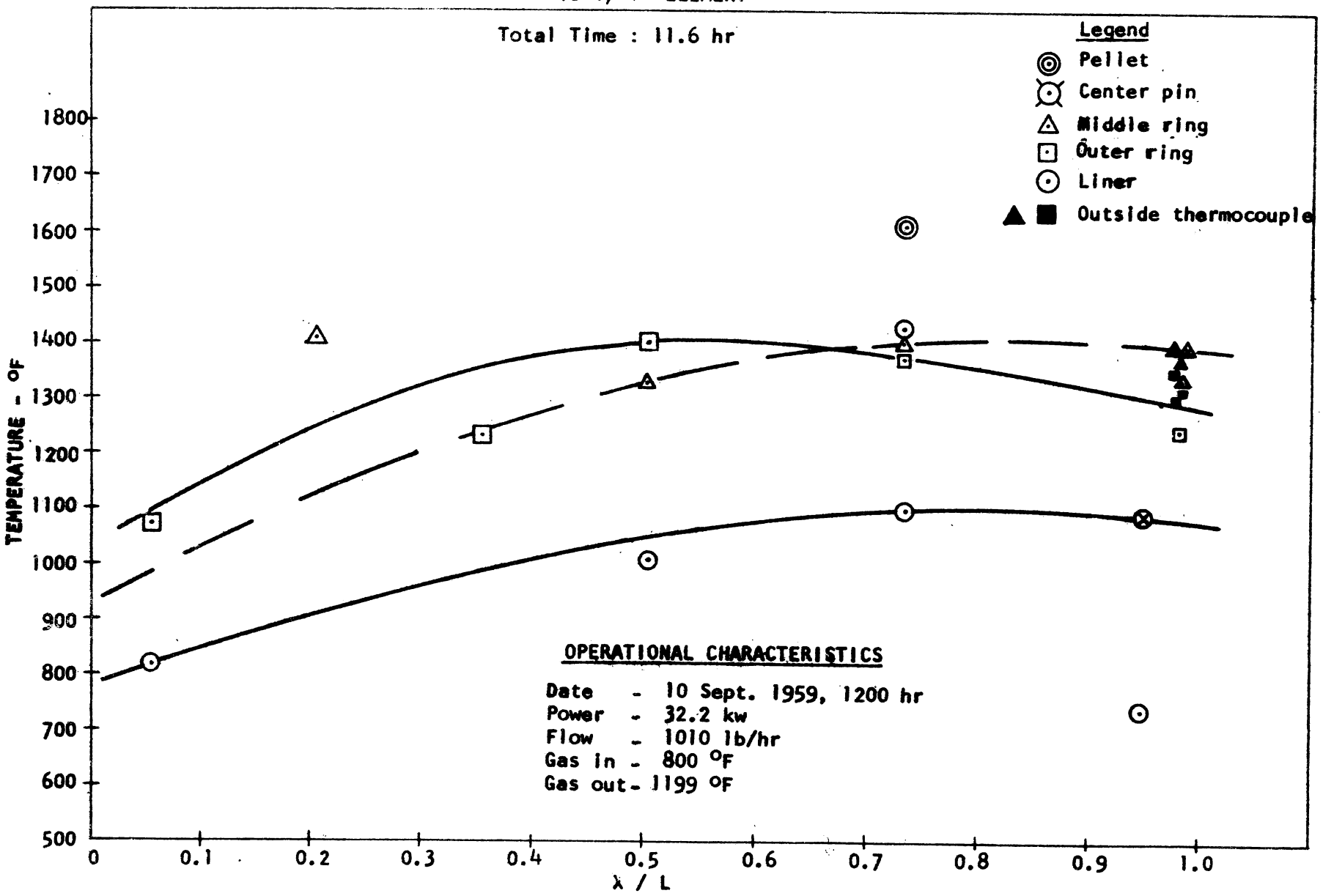

Figure IV-4

TEMPERATURE PROFILE
IB-1βT ELEMENT

Total Time : 26.0 hr

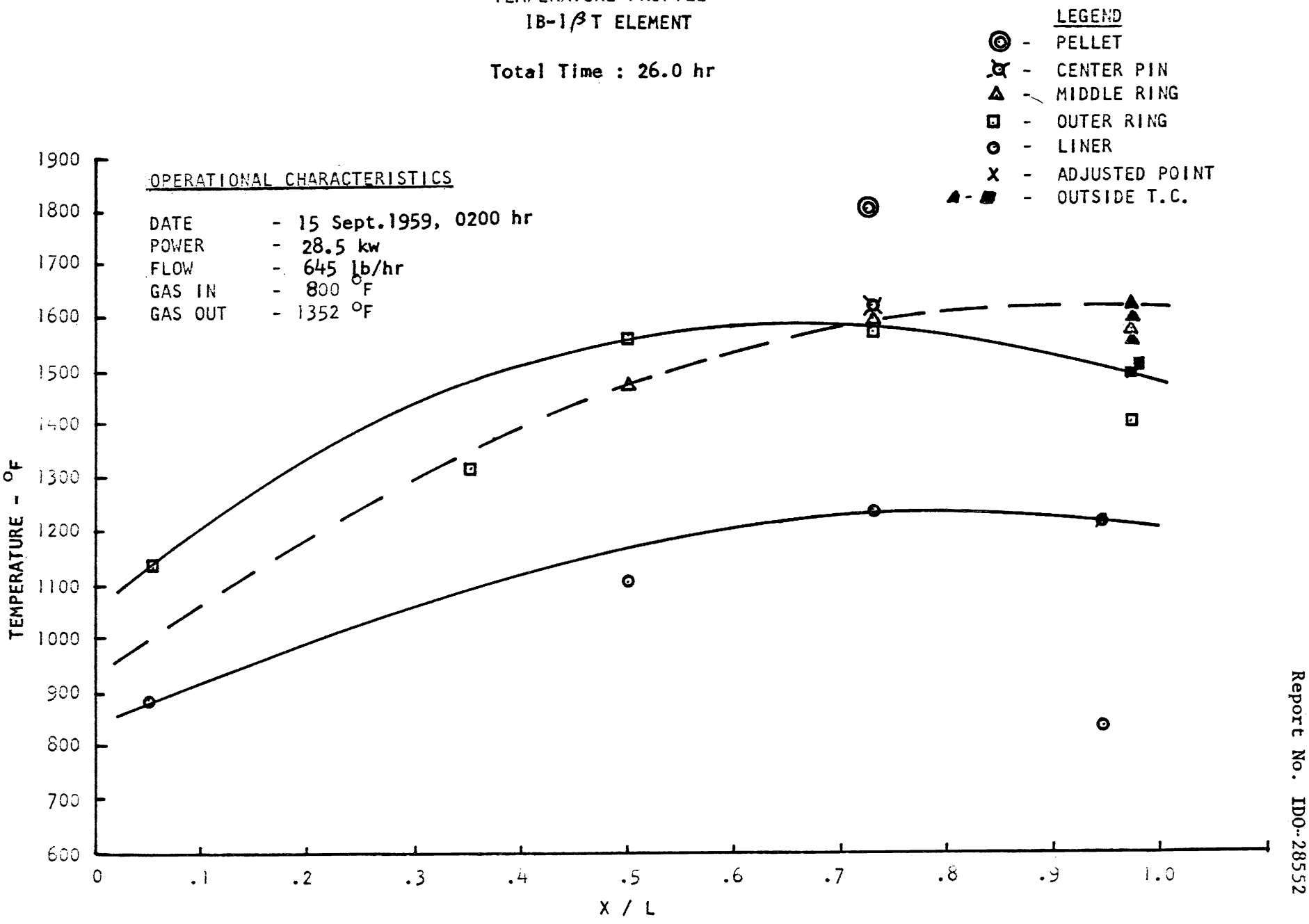

Figure IV-5

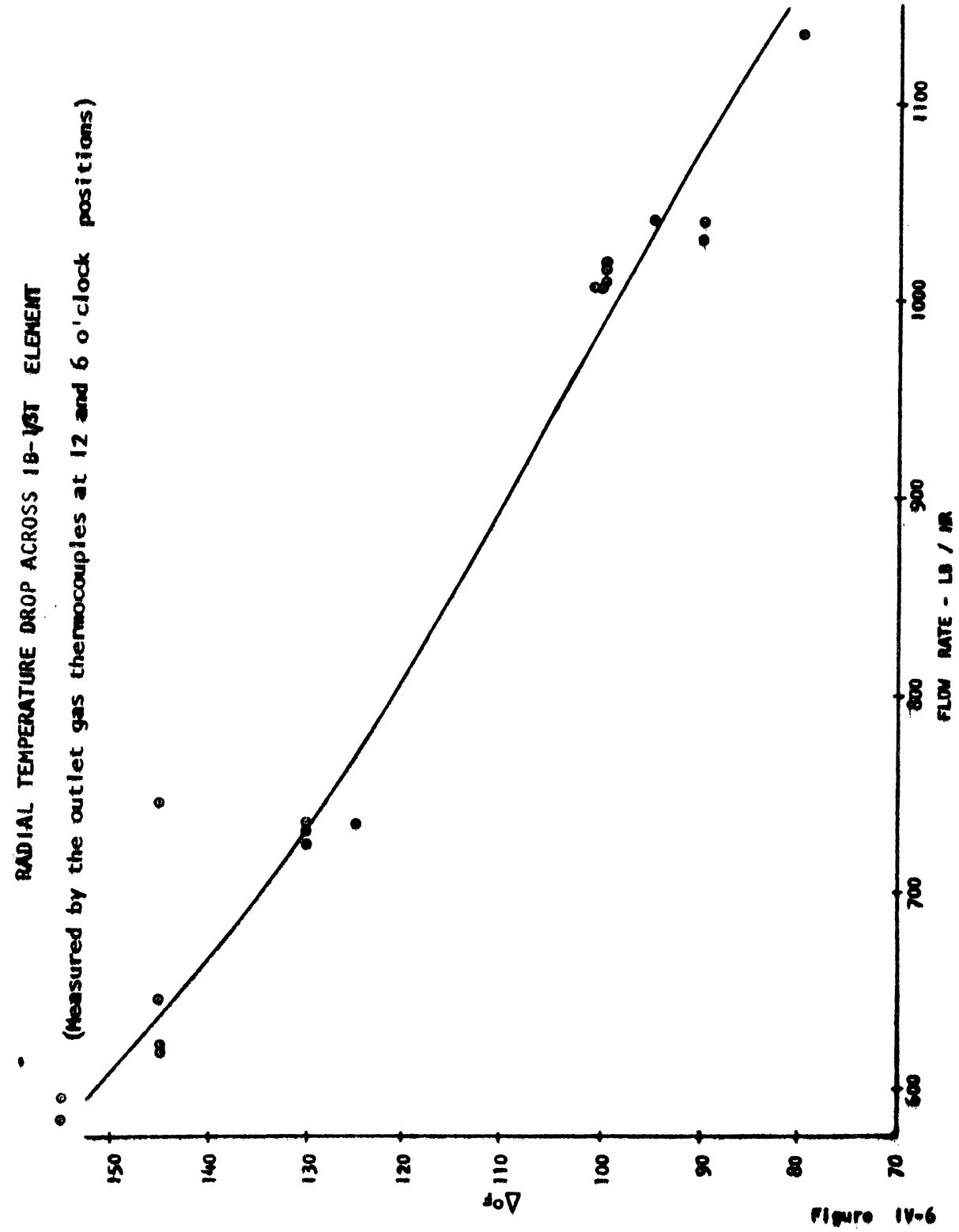
RADIAL TEMPERATURE DROP ACROSS 18-INCH ELEMENT
(Measured by the outlet gas thermocouples at 12 and 6 o'clock positions)
ΔT°F
150
140
130
120
110
100
90
80
70
600
700
800
900
1000
1100
FLOW RATE - LB / HR

Figure IV-6

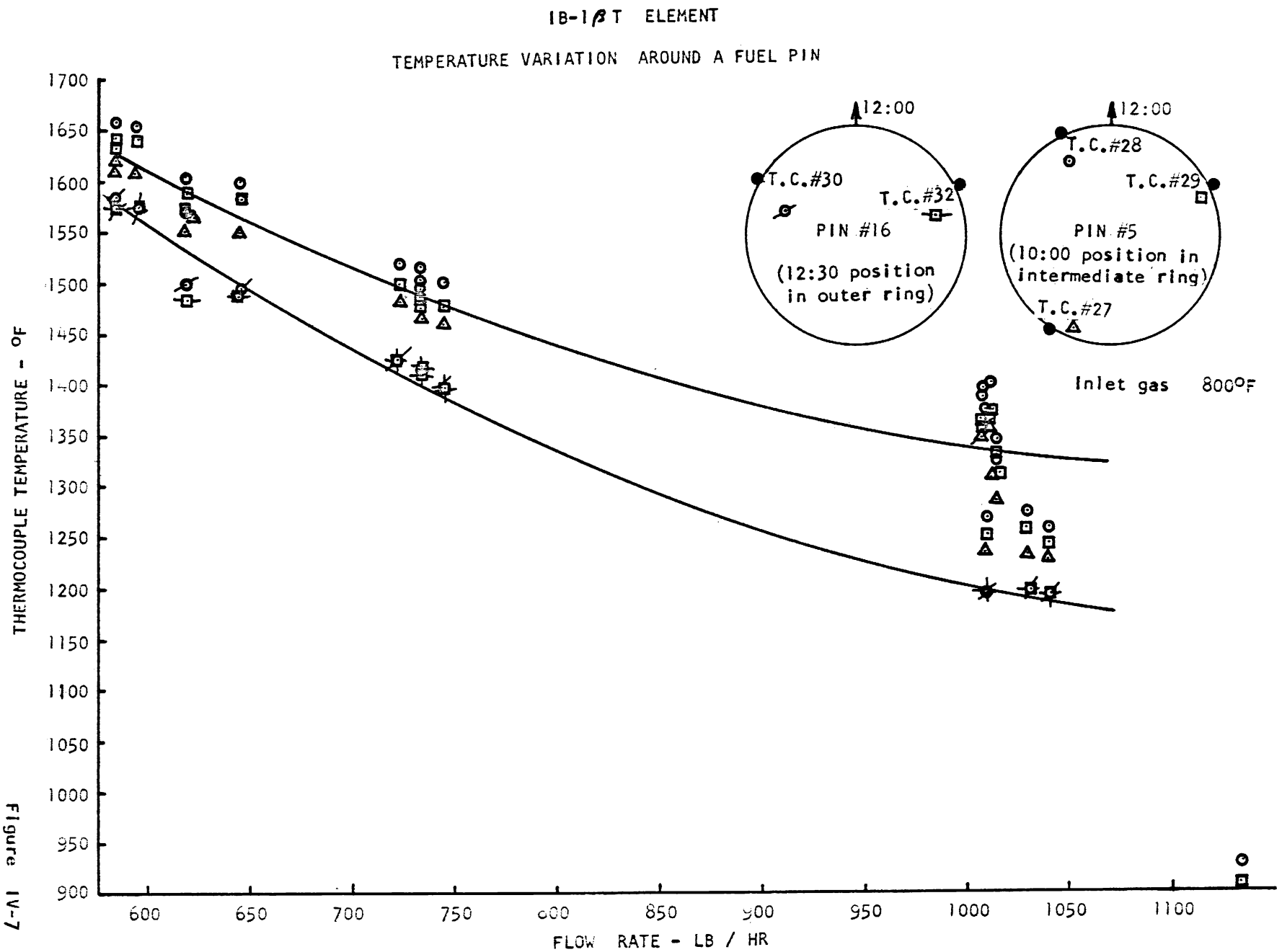
1B-1βT ELEMENT
TEMPERATURE VARIATION AROUND A FUEL PIN
THERMOCOUPLE TEMPERATURE - °F
FLOW RATE - LB / HR
12:00
T.C.#30
T.C.#32
PIN #16
(12:30 position in outer ring)
12:00
T.C.#28
T.C.#29
PIN #5
(10:00 position in intermediate ring)
T.C.#27
Inlet gas 800°F

Figure IV-7

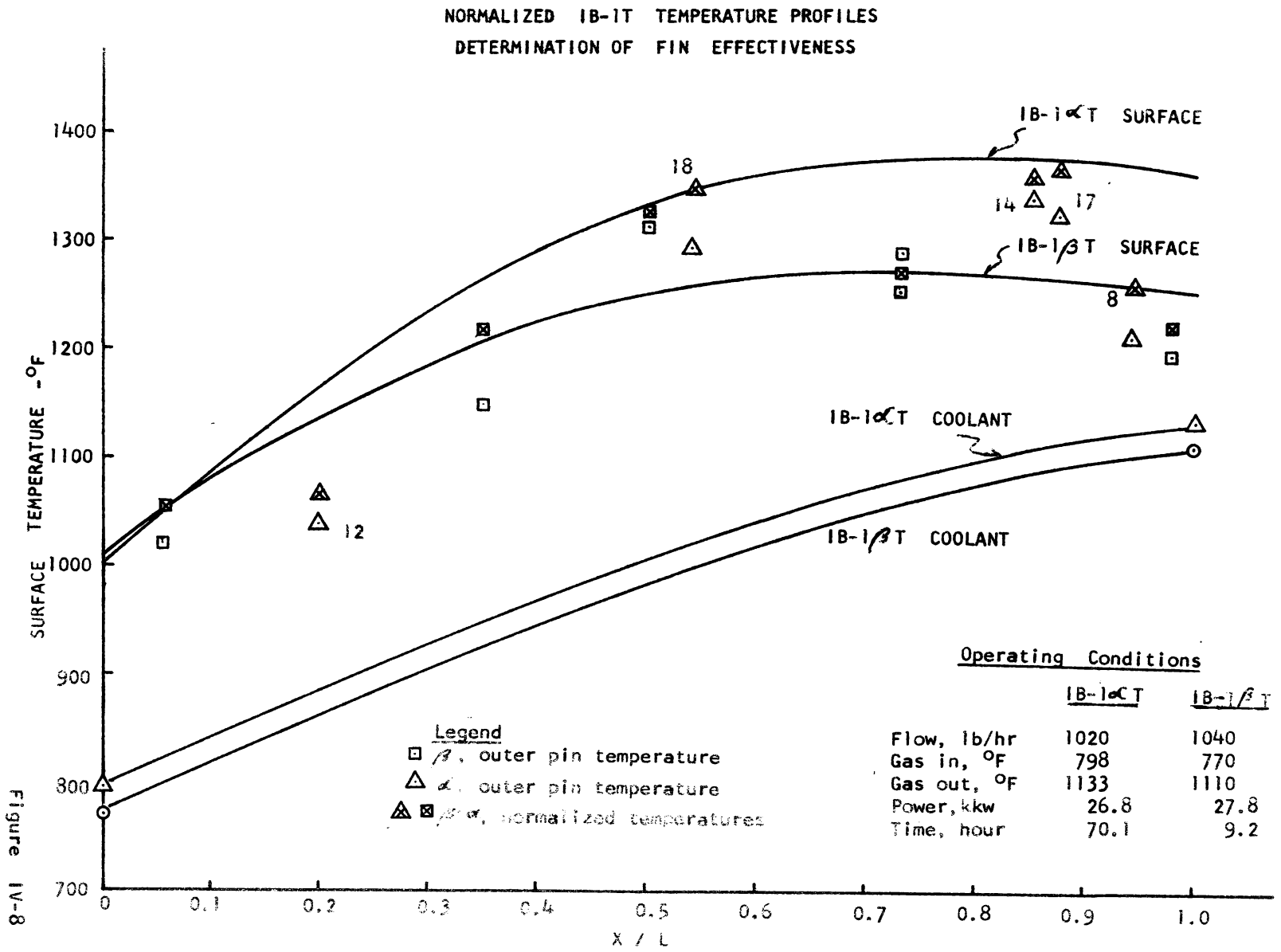
NORMALIZED 1B-1T TEMPERATURE PROFILES
DETERMINATION OF FIN EFFECTIVENESS
1B-1∝T SURFACE
1B-1β T SURFACE
1B-1∝T COOLANT
1B-1β T COOLANT
SURFACE TEMPERATURE - °F
X / L
1400
1300
1200
1100
1000
900
800
700
0
0.1
0.2
0.3
0.4
0.5
0.6
0.7
0.8
0.9
1.0
18
14
17
8
12
Legend
β, outer pin temperature
∝, outer pin temperature
β ∝, normalized temperatures
Operating Conditions
1B-1∝T
1B-1β T
Flow, lb/hr 1020 1040
Gas in, °F 798 770
Gas out, °F 1133 1110
Power, kkw 26.8 27.8
Time, hour 70.1 9.2

Figure IV-8

NORMALIZED IB-1T TEMPERATURE PROFILES
DETERMINATION OF FIN EFFECTIVENESS

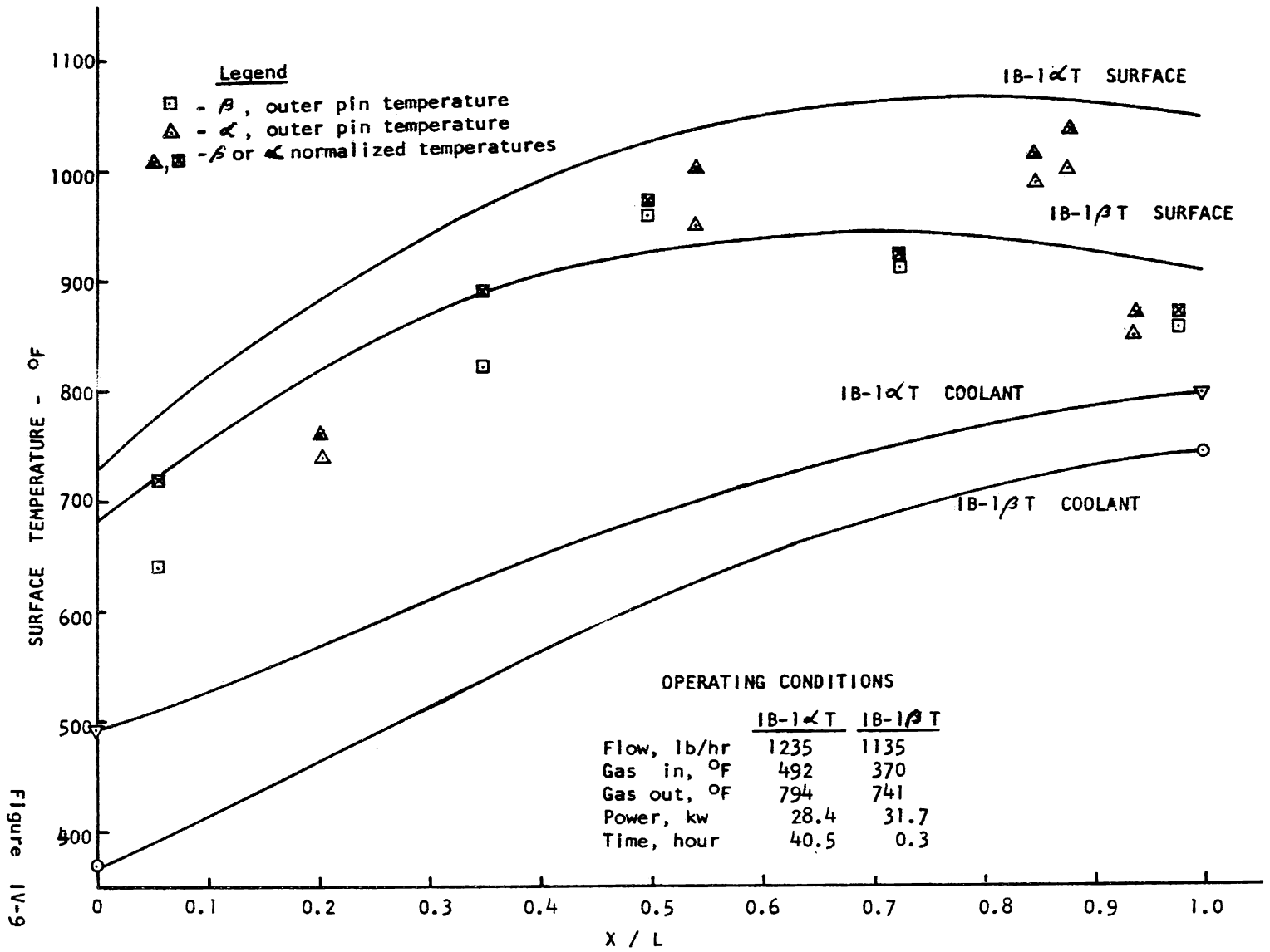

OPERATING CONDITIONS

	IB-1∝T	IB-1βT
Flow, lb/hr	1235	1135
Gas in, °F	492	370
Gas out, °F	794	741
Power, kw	28.4	31.7
Time, hour	40.5	0.3

Figure IV-9

EXPERIMENTAL PRESSURE DROP VERSUS FLOW RATE

IB - 1βT FUEL ELEMENT

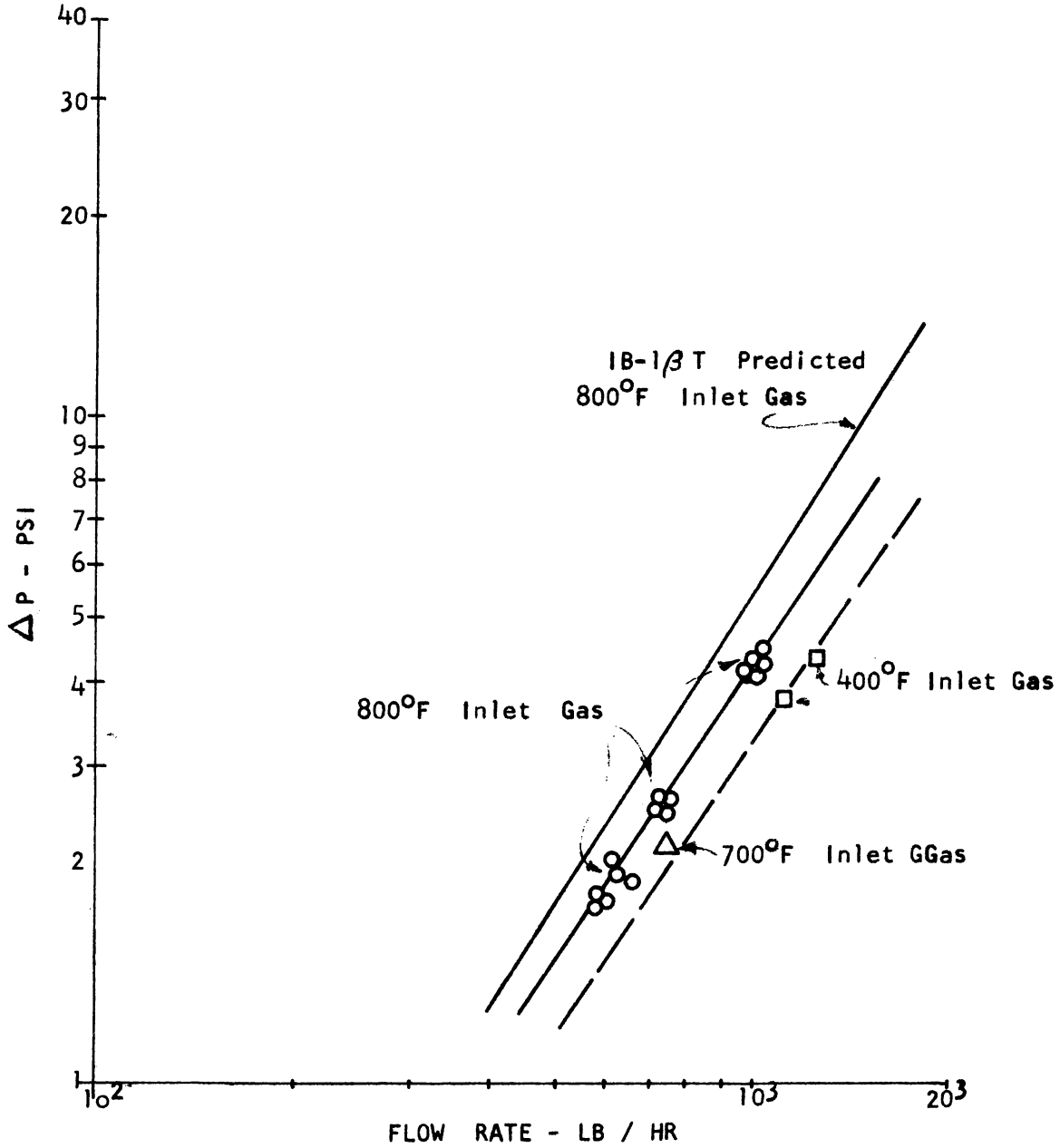

Figure IV-10

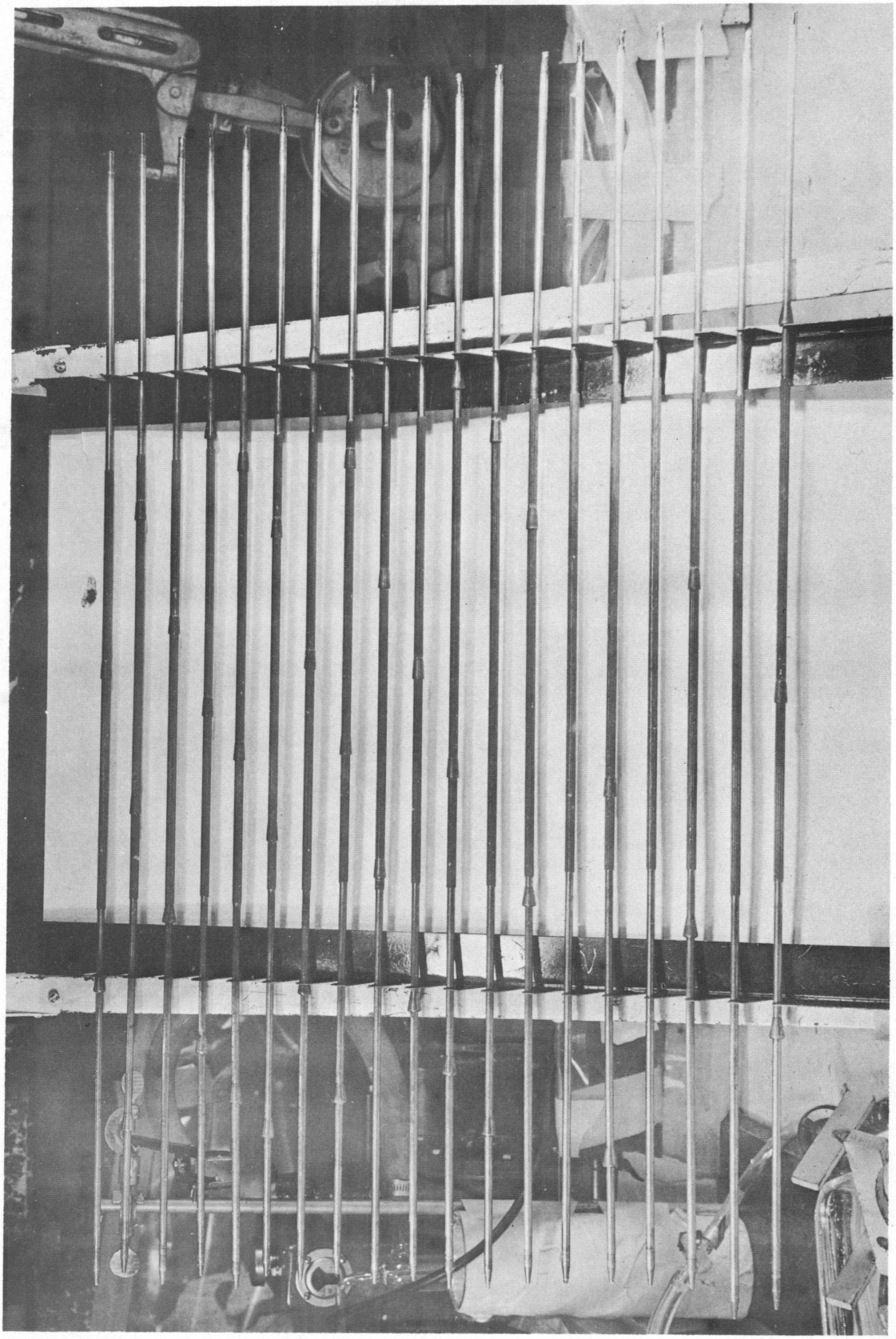

FUEL PINS
IB-1/βT FUEL ELEMENT

Figure IV-11

V. FLUX MAPPING

The thermal neutron flux in the IB-1ØT fuel element was measured on July 28, 1959. The IB-1ØT, a nuclear mockup of the power elements, with identical fuel pellets and tubing material, was inserted in the BRR-GCR loop, pressurized to 80 psig, and irradiated for 5 min at a power level of 400 watts. (Refer to Section II. B. 3, IB-1ØT Test Element and to Figure II-4).

After irradiation, the element was allowed to "cool" for 3 hr before axially located counting wires (Mn-Cu composition) and the gold foil were removed. The wires were cut into one-inch segments and counted.

Pins 1, 4, 7, 9, and 15 were taken from the element, and wires wrapped around removable sections of each pin were removed, cut into four segments, and counted. The counting values were normalized to the count from the axial wire corresponding to the center of Pin 1, and the activity was plotted at the mid-point of the respective section. The flux variation around a fuel pin, shown in Figure V-1, varies by a factor of about two, except in the central pin. The capsule sections were removed from each pin and counted. The relative activity of these capsules is shown in Figure V-2 as the lower number of the respective pin.

The axial flux distributions are shown graphically in Figure V-3, for Pins 2 and 10. The averaged flux of all of the pins is shown in Figure V-4. As seen from these graphs, a sizeable flux peaking occurs above the fuel region of the pins. The peak is not attenuated appreciably from the outer to the inner pins. Since the region above the fueled portion of the pins is occupied by gas and by Inconel tubing, this peak is probably a reflection of the axial reflector peak of the BRR core, which occurs at approximately the same vertical location. Examination of the data showed that the element had apparently been rotated approximately 90 degrees during insertion into the loop.

Figure V-2 shows that there was a 24.5% decrease in flux from the high flux side to the low flux side of the outer ring. The axial peak-to-average flux ratio over the fueled length was very nearly constant for all 19 pins. The average ratio was 1.24, with local deviations up to 0.03.

The thermal neutron flux was measured with the gold foil. A cadmium ratio of 2.48 was assumed. With this assumption, the thermal neutron flux at the gold foil position was 4.96×10^{12} n/cm^2-sec, at 2 Mw reactor power.

Flux depressions in the pins were obtained by taking the ratio of center pin flux to the average surface flux. This gave an average flux depression of 0.50 for the outer pins and 0.36 for the inner pins.

CIRCUMFERENTIAL FLUX DISTRIBUTIONS

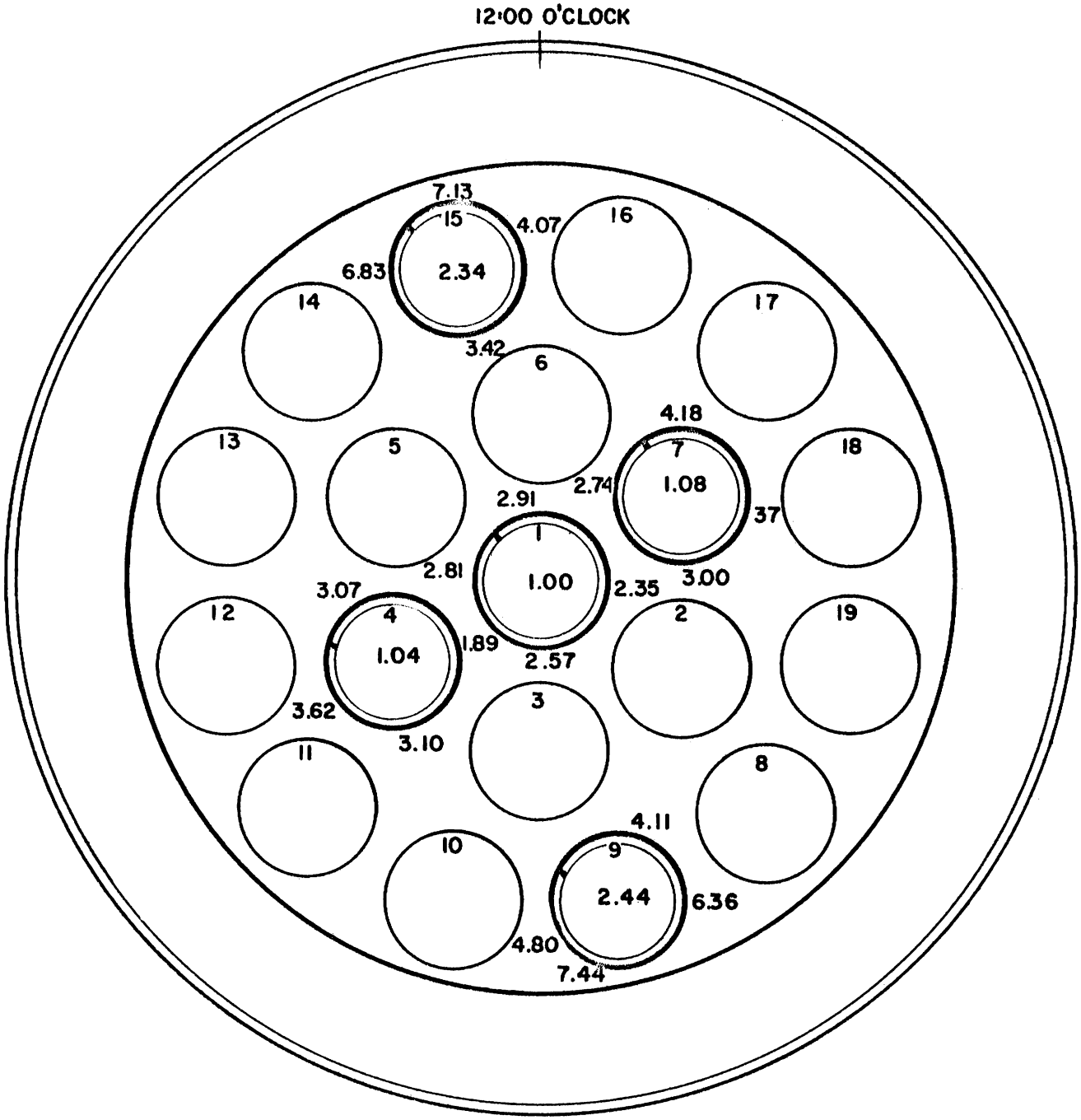

Figure V-1

AVERAGE FUEL-WEIGHTED FLUX DISTRIBUTION AND RELATIVE CAPSULE ACTIVITIES

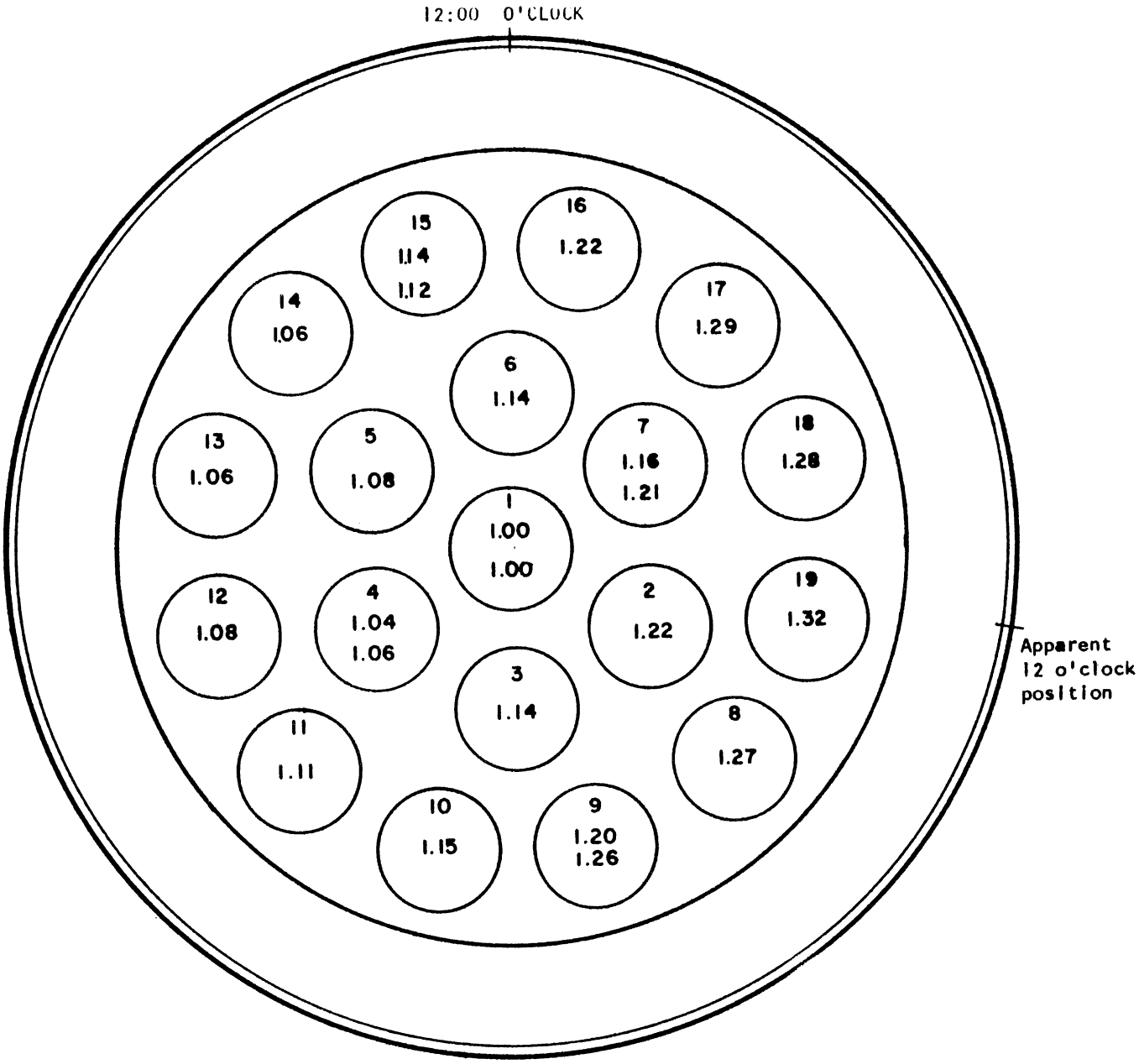

Figure V-2

AXIAL FLUX DISTRIBUTION (PINS 2 AND 10)

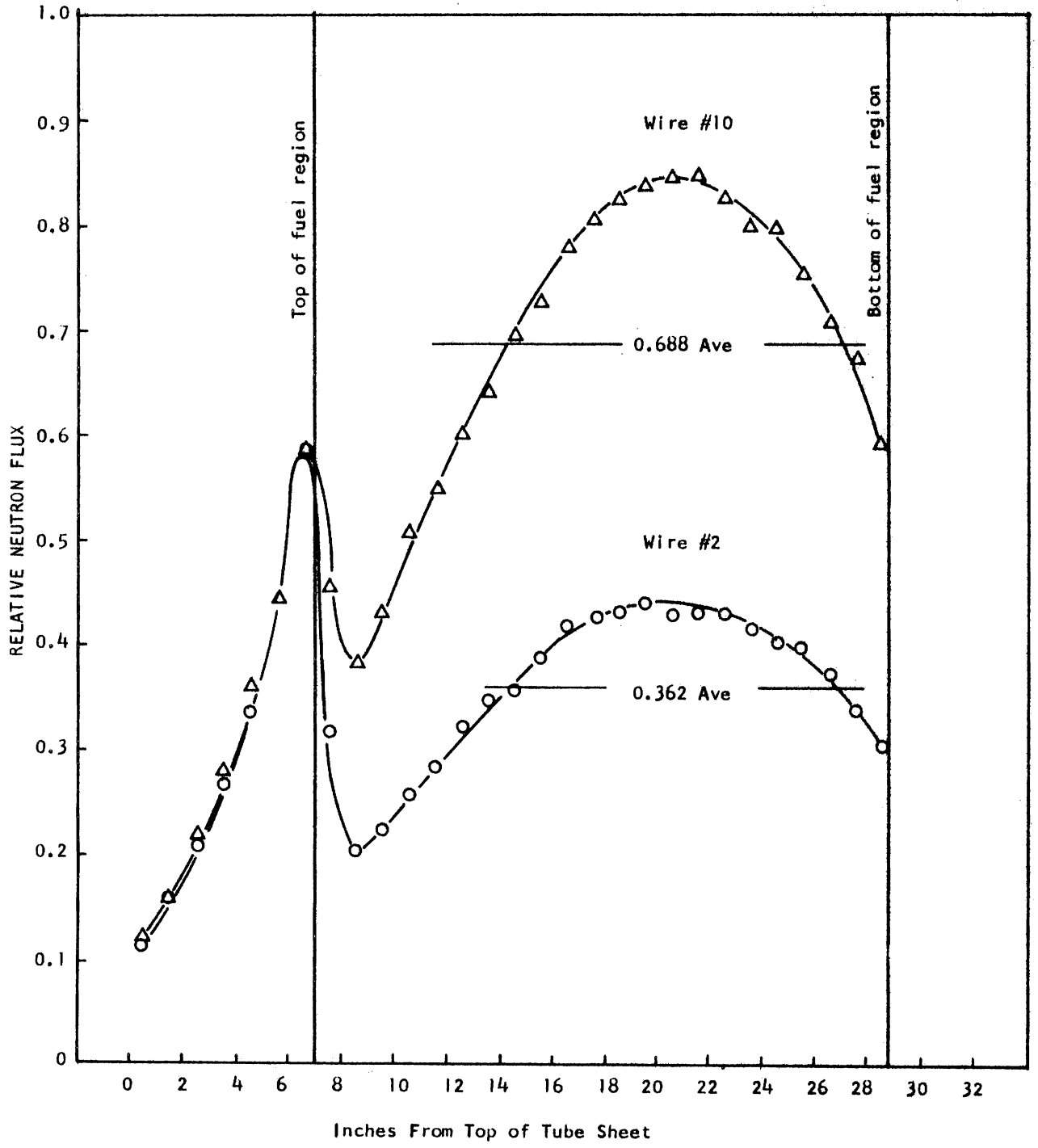

Figure V-3

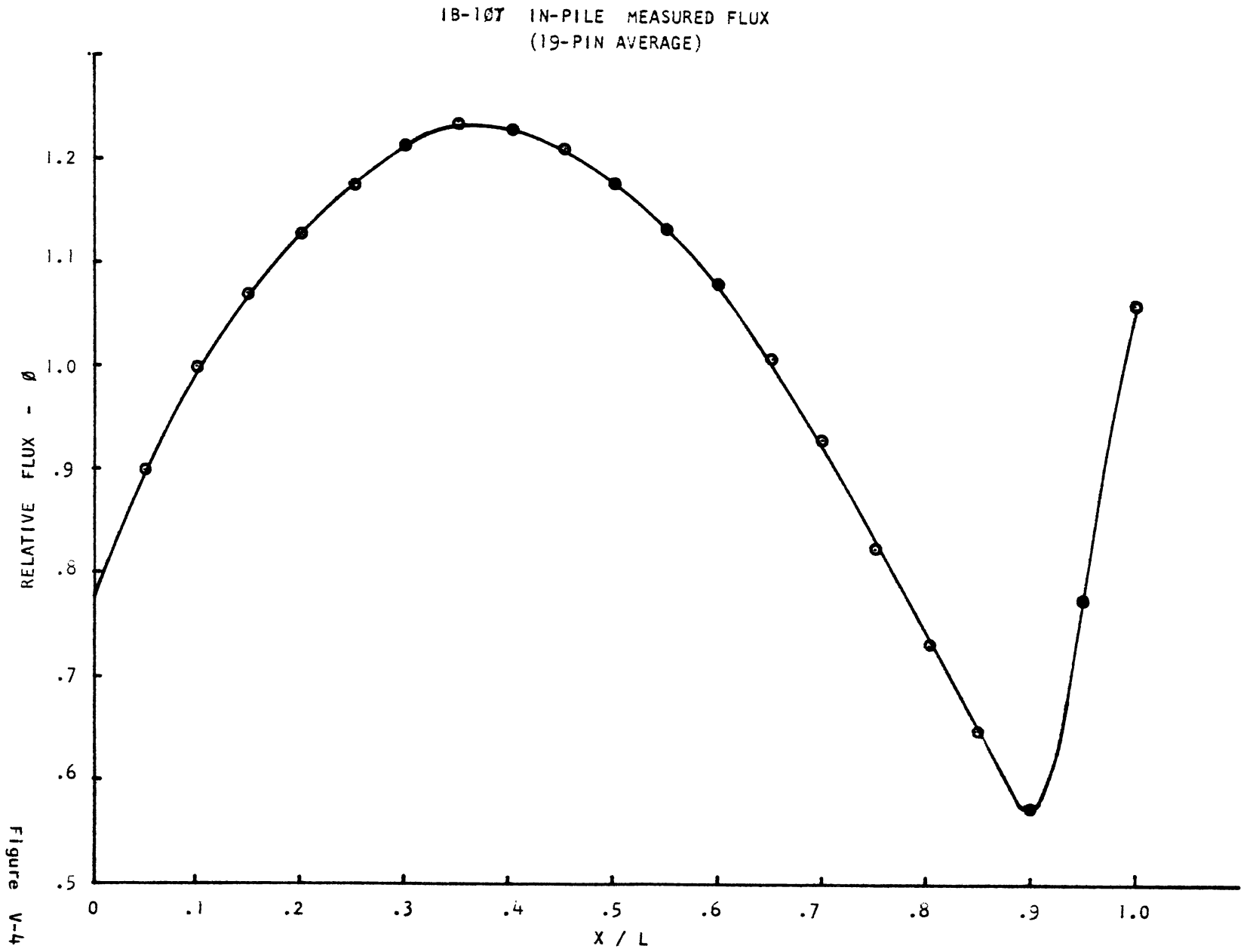
IB-10T IN-PILE MEASURED FLUX
(19-PIN AVERAGE)
RELATIVE FLUX - ø
1.2
1.1
1.0
.9
.8
.7
.6
.5
0
.1
.2
.3
.4
.5
.6
.7
.8
.9
1.0
X / L

Figure V-4

VI. CONCLUSIONS AND FUTURE WORK

A. CONCLUSIONS

Results from the series of tests made to date indicate that present theory for predicting the IB fuel element performance requires some refinement.

Data for heat transfer and fluid flow evaluations could not be refined because of fission breaks in the fuel element during the irradiations. Some qualitative conclusions were reached:

1 Enrichment of the UO_2 fuel in the outer ring of pins is close to the optimum value for the loop conditions.

2 Friction factors are in fair agreement with those measured in out-of-pile water flow tests.

3 The use of fins on the fuel pins did not significantly increase the heat transfer capability.

Significant distortions in the element did not develop as a result of thermal cycling. The fuel element appears to be well designed from this viewpoint.

Considerable development work must be done to achieve mechanical integrity of the fuel pins.

B. FUTURE WORK

Presently a second test of the IB fuel element, designated the IB-2T, is being planned. Fabrication of the test element is nearly complete, and in-pile testing will be initiated in the near future. This element will utilize larger diameter pins (0.241 in. diameter versus the 0.225 in. IB-1T pins). Enrichment of UO_2 in the outer circle of fuel will be increased to 33%. A third test, the IB-4T, utilizing BeO as a diluent in fully enriched UO_2, is being initiated.

Several different methods of radially positioning the fuel pins are being investigated. The IB-2T and IB-4T elements will use wires, spirally wrapped around the fuel pin, as spacers.

BIBLIOGRAPHY

References

(1) Bodnar, George T., et al, An In-Pile Gas-Cooled Loop Installed at the Battelle Research Reactor, BMI-1290, September 1958.

(2) Reynolds, W.C., Computing Routine for Calculating Temperatures in Two-, Three-, or Four-Plate Reactor Fuel Element; AGN TM-332, August 1958.

(3) Mackewicz, W. V., and Wilber, W. W., Water Flow Tests, AGN Note 681, January 1959.

Literature Consulted

Watanabe, H. T., et al., Description of IB-1T Fuel Element In-Pile Experiment, AGN TM-345, January 1959; and Addendum to AGN-345, April 1959.

Basham, S. J., and Francis, G. A., Irradiation of AGN IB-1αT Fuel Element Subassembly in BRR In-Pile Recirculating Gas Loop, Battelle Memorial Institute, September 1959.

Basham, S.J., and Francis, G. A., Irradiation of the AGN IB-1βT Fuel Element Subassembly in BRR In-Pile Recirculating Gas Loop, Battelle Memorial Institute, September 1959.

Fairand, B. P., and Anno, J. N., Flux Measurements with the IB-1ØT Fuel Element, Battelle Memorial Institute, September 1959.

Reynolds, W.C., Analysis of Internal Pin Thermocouple Temperatures, AGN-HFED Notes 126 and 126A, November 1959.

Titus, G. W., Hot-Cell Results from IB-1αT Examination, AGN-HFED Memorandum 1, January 1960.